OKLAHOMA STATE UNIVERSITY

SECOND-HARMONIC GENERATION AND

OPTICAL MIXING PROCESSES

By

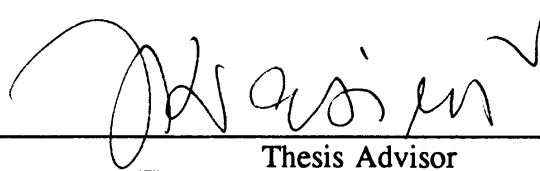PRANAV B. DOSHI

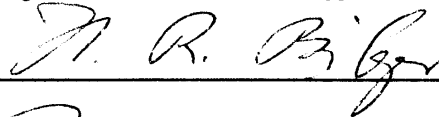Bachelor of Engineering

University of Bombay

Bombay, India

1990

Submitted to the Faculty of the
Graduate College of the
Oklahoma State University
in partial fulfillment of
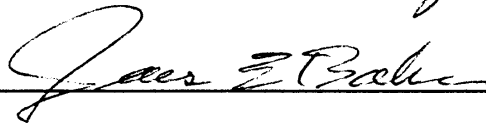the requirements for
the Degree of
MASTER OF SCIENCE
May, 1993

SECOND-HARMONIC GENERATION AND
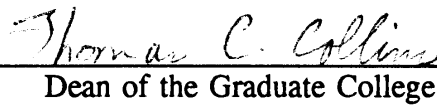
OPTICAL MIXING PROCESSES

Thesis Approved:

_____
Thesis Advisor

_____

_____

_____
Dean of the Graduate College

PREFACE

At the OSA Annual Meeting held at Albuqurque, NM, September 1992, Dr. Y. R. Shen was awarded the Schawlow Prize. His award winning paper was on Reflection on Nonlinear Reflection. He had reviewed the status of surface and interface studies by optical second harmonic and sum-frequency generations. There were also many other presentations in that conference on nonlinear optics, especially on second harmonic and sum or difference frequency generations.

The basis of most of the recent advances in the field of lasers and optics is a thorough knowledge of nonlinear optics. Nonlinear optics has got a very bright future especially in the research arena. An attempt has been made to review the theories of linear and nonlinear optics, with a focus on parametric conversions. A few nonlinear materials have been cited in this work. An experiment to improve the efficiency of sum-frequency generation for broadband inputs performed in this laboratory has been discussed at length.

I would like to express my sincere gratitude to my major advisor, Dr. Jerzy Krasinski, whose inspiration, guidance, and constant encouragement kept me motivated during this research project. I appreciate his endless amount of time and effort in this work. I am also thankful to Dr. Hans Bilger for assisting me throughout my courses in the field of optics, and Dr. James Baker for serving on my committee.

Dr. C. Radzewicz, a visiting professor from Poland, helped me throughout his stay at Stillwater. I deeply appreciate the efforts that he has put in to improve my theoretical as well as the practical knowledge. Special thanks go to Gary Pearson who guided me throughout my studies and helped to overcome the difficulties.

I extend my sincere thanks to all my friends in Stillwater and outside for their everlasting support.

Finally, I owe a deep sense of gratitude to my parents, Jyoti and Bharat Doshi, my sister Binita, and my wife Shefali for patiently providing unending support and encouragement throughout my graduate studies at Oklahoma State University.

TABLE OF CONTENTS

LIST OF FIGURES

NOMENCLATURE

c	Velocity of light in free space (vacuum)
d	Thickness of the material
e	Charge of an electron
E	Applied electric field
$E(\omega)$	Complex amplitude of the electric field
k	Propagation constant or Wave vector
m	Mass of an electron
n	Absolute refractive index of the material
N	Number of atoms
r	Displacement of the electron from its equilibrium position
S	Poynting vector
s	Unit vector normal to the wavefront
W	Stored energy density
γ	Damping constant
$\Delta\omega$	Linewidth
ε	Dielectric permittivity
ε_0	Dielectric permittivity of vacuum
μ	Magnetic Permeability

μ_0	Magnetic Permeability of vacuum
ξ	Anharmonicity
τ	Time, phase decay time
χ	Susceptibility
ω	Angular frequency
ω_o	Natural angular frequency of the electron
ϑ	Frequency
E_R	Real amplitude of the electric field

CHAPTER I

INTRODUCTION

1.1 Overview

"Physics would be dull and life most unfulfilling if all physical phenomena around us were linear. Fortunately, we are living in a nonlinear world. While linearization beautifies physics, nonlinearity provides excitement in physics." [21]

With the advent of lasers, which provide a source of high-intensity coherent light, much progress has been made in the field of nonlinear optics. The strong oscillating electric field of the laser beam creates a polarization response that is nonlinear in character and that can act as a source of new optical fields with altered properties. The most important of all these nonlinear optical processes is the second-harmonic frequency generation. This frequency doubling process has wide applications. It converts the light from near-infrared region to deep blue. Since the size of the focussed spot of light is inversely proportional to its wavelength, second-harmonic generation can increase the capacity of stored information on optical disks immensely. Parametric conversion processes like sum and difference-frequency generation can be applied to build devices such as frequency mixers or up or down converters, that can act as new light sources or as amplification schemes.

1

1.2 Objectives

The literature on nonlinear optical phenomena has been expanding rapidly. A complete survey of the work to date is beyond the scope of this thesis. Recognizing this, an attempt has been made to present an outline of the theoretical treatment so as to catalog the various effects, and to review the experimental work done in our laboratory.

Theories involved in linear and nonlinear optics differ mainly due to introduction of terms involving nonlinearities of polarization. Chapter II describes the linear optical effects. It discusses the physical origin of the linear refractive index and the propagation of light in isotropic and anisotropic media. The theory of nonlinear optical interactions is introduced in chapter III. It gives an introduction of second harmonic and sum-difference frequency generation concepts. The higher efficiency of conversion are very essential, and that could be achieved by proper phase matching. This is discussed in chapter IV which includes the various phase-matching techniques. Second-order nonlinear optical processes are a major part of this thesis, and they have been explained in detail in chapter V. The concept of multimode laser for generation of parametric frequencies is also discussed. An experiment to increase the efficiency of sum-frequency generation for broadband input fields, which was performed in our lab, is described in this thesis. The efficiency was improved by introducing a time delay between two or more nonlinear mixing crystals. Chapter VI summarizes the overall work and concludes the present day advantages and future prospects of research in the field of nonlinear optics. At the end, the nonlinear optical properties of classical and

recent uniaxial as well as biaxial crystals are given in the appendix. The c.g.s. system

is used throughout this thesis for derivations and other purposes to avoid any

confusions.

CHAPTER II

AN OVERVIEW OF LINEAR OPTICS

2.1 Lorentz Model

Let us consider a classical Lorentz model which consists of a single atom with

one electron and a nucleus [26]. Whenever an electric field is applied to it, the

distance between the electron and the nucleus changes which induces polarization. An

alternating electric field will induce an alternating polarization of the same frequency.

The oscillating dipole thus formed radiates an electromagnetic wave, with a phase

dependent on the restoring force between the electron and the nucleus.

Let us consider a string of N such atoms in row, such that the resultant wave

coming out of each atom is different in phase than the incident wave. This wave is

made incident on the next atom to give a final electromagnetic wave with a different

phase which is dependent on the number of atoms and their properties due to these

types of interactions. If 'd' is the thickness of the material which in turn is proportional

to the number of atoms N, then the ratio of velocity of the incident wave not passing

through the material and the velocity of the same wave when made to pass through the

material gives the absolute refractive index of the material.

The radiation pattern of the oscillating dipole has a $\sin\theta$ term in it, depending

on the type of radiation. Since the radiations in any direction other than the forward direction result in a destructive interference, it gives rise to a refractive index. But there is a tendency of incoherent scattering in impure materials. Also, the vibrations of the atoms with each other heat up the material, and a part of the energy is absorbed. To analyze this mathematically, we write

$$\frac{d^2r}{dt^2} + 2\gamma\frac{dr}{dt} + \omega_0^2 r = -\frac{e}{m}E \qquad (2.1)$$

as the equation of motion for an electron oscillating around its equilibrium position, where r is the displacement of the electron from its equilibrium position, e is the charge of the electron, m is its mass, ω_0 is its natural frequency, γ is the damping constant and E is the applied electric field.

Let the electric field be given as

$$E = E_R \cos(\omega t - \varphi)$$

In the complex notation this can be written as

$$E = E(\omega)e^{-i\omega t} + E^*(\omega)e^{i\omega t}$$

where

$$E(\omega) = \frac{1}{2}E_R e^{i\varphi}$$

and

$$E^*(\omega) = \frac{1}{2}E_R e^{-i\varphi} = E(-\omega)$$

On substituting this in equation 2.1 gives the solution for a linear equation.

$$r = -\frac{e}{m}E(\omega)\,\frac{e^{-i\omega t}}{\omega_0^2-2i\gamma\omega-\omega^2} + complex\ conjugate$$

Polarization density is P = -Ner

$$\therefore P=\frac{Ne^2}{m}\,\frac{1}{\omega_0^2-2i\gamma\omega-\omega^2}E(\omega)\,e^{-i\omega t} + complex\ conjugate \quad (2.2)$$

Let

$$\chi(\omega)=\frac{Ne^2}{m}\,\frac{1}{\omega_0^2-2i\gamma\omega-\omega^2} \quad (2.3)$$

Hence

$$P = \chi(\omega)E(\omega)\,e^{-i\omega t} + complex\ conjugate \quad (2.4)$$

Thus we find that the induced polarization is proportional to the amplitude of the applied alternating field and has the same frequency.

By putting the polarization as a source term in Maxwell's equations we get [4, 26]

$$\nabla\times H=\frac{1}{c}\frac{\partial D}{\partial t}+\frac{4\pi}{c}\,j \quad (2.5)$$

$$\nabla\times E=-\frac{1}{c}\frac{\partial}{\partial t}\,(\mu H) \quad (2.6)$$

where

$$D=E+4\pi P$$

Hence

$$\nabla \times H = \frac{4\pi\sigma}{c} E + \frac{1}{c} \frac{\partial(\varepsilon E)}{\partial t}$$

where σ is the conductivity and $\varepsilon = (1 + 4\pi\chi)$

For a nonconducting and a nonmagnetic material $\sigma = 0$ and $\mu = 1$

Taking curl on both sides of the equation 2.6

$$\nabla \times \nabla \times E = \nabla \times \left(-\frac{1}{c} \frac{\partial}{\partial t} \mu H \right)$$

$$\nabla \nabla \cdot E - \nabla^2 E = \nabla \times \left(-\frac{1}{c} \frac{\partial}{\partial t} H \right)$$

But

$$\nabla \cdot E = 0$$

$$\therefore -\nabla^2 E = -\frac{1}{c} \frac{\partial}{\partial t} (\nabla \times H)$$

$$\therefore \nabla^2 E = \frac{1}{c} \frac{\partial}{\partial t} \left(\frac{1}{c} \frac{\partial \varepsilon E}{\partial t} \right)$$

$$\therefore \nabla^2 E = \frac{\varepsilon}{c^2} \frac{\partial^2 E}{\partial t^2}$$

For one dimensional situation

$$\frac{d^2 E}{dz^2} = \frac{\varepsilon}{c^2} \frac{\partial^2 E}{\partial t^2} \qquad (2.7)$$

Let the solution for the above equation be

$$E(z, t) = E_R e^{i(\omega t - kz)} + complex\ conjugate \qquad (2.8)$$

Hence

$$k^2 = \frac{\varepsilon\omega^2}{c^2}$$

Here k is the propagation constant of the material. k is a function of the wave as well as its velocity in the material. But the velocity is determined by the refractive index of that material.

Hence k = nω/c

and

$$n^2 = \varepsilon = 1 + 4\pi\chi \tag{2.9}$$

On substituting equation 2.3 in 2.9 we get

$$n^2 = 1 + \frac{Ne^2}{m} \frac{4\pi}{\omega_0^2 - 2i\gamma\omega - \omega^2} \tag{2.10}$$

When $\gamma = 0$ i.e. no damping, n is a real quantity and is dependent on frequency, while for $\gamma \neq 0$, n is complex. The imaginary part is the measure of absorption and is very large in the vicinity of ω_0^2. In most of the materials there is more than one natural frequency ω_0 and therefore more than one absorption bands exist. The absorption caused by the electron transitions give higher natural frequency lying in the ultraviolet and visible region of the spectrum. But if the frequency is the natural resonance of vibration of the atoms with respect to each other, then the frequency is low and lies in the infra-red band. Usually there are several different groups of atoms in the crystal, hence the absorption spectrum can give the direct information about those groups of atoms. Otherwise if the composition of a material is

known, the region in which it will be absorbing can be predicted.

2.2 Anisotropy

The natural frequency ω_0 and the refractive index of a material are dependent on the interaction between the atoms. But this interaction does not remain the same in all the directions. Thus such a medium is called anisotropic. Such a phenomenon mostly occurs in crystals. In such crystals the dielectric constant is a tensor. This second rank tensor relates the dielectric displacement in one direction to the field in each of the three directions.

$$D_i = \varepsilon_{ij} E_j \tag{2.11}$$

Let us carry the following assumptions from the isotropic case.

The energy flux is given by the Poynting vector where the electric field and the magnetic field contains each half of the energy [26].

The stored electric density is

$$W_e = \frac{1}{8\pi} (E \cdot D) \tag{2.12}$$

$$W_e = \frac{1}{8\pi} (E_j \varepsilon_{jk} E_k) \tag{2.13}$$

Hence,

$$\frac{\partial}{\partial t} (W_e) = \frac{1}{8\pi} (E_k \varepsilon_{kj} \frac{\partial E_j}{\partial t} + E_j \varepsilon_{jk} \frac{\partial E_k}{\partial t}) \tag{2.14}$$

From the Poynting Vector Theorem,

$$S = \frac{c}{4\pi} (E \times H)$$

The net power flow out of a unit volume is

$$\nabla \cdot S = \frac{c}{4\pi} \nabla \cdot (E \times H) \tag{2.15}$$

On substituting from equations 2.5 and 2.6

$$\nabla \cdot S = \frac{E \cdot (\frac{\partial D}{\partial t}) + H \cdot (\frac{\partial H}{\partial t})}{4\pi} \tag{2.16}$$

Using equation 2.11

$$\nabla \cdot S = \frac{1}{4\pi} (E_k \varepsilon_{kl} \frac{\partial E_l}{\partial t} + H \frac{\partial H}{\partial t}) \tag{2.17}$$

On equating the electric energy density terms of equations 2.14 and 2.13 we get

$$\frac{1}{4\pi} (E_j \varepsilon_{jk} \frac{\partial E_k}{\partial t}) = \frac{1}{8\pi} (E_k \varepsilon_{kj} \frac{\partial E_j}{\partial t} + E_j \varepsilon_{jk} \frac{\partial E_k}{\partial t})$$

which gives $\varepsilon_{jk} = \varepsilon_{kj}$

Thus the tensor is symmetrical.

Rewriting equation 2.12 we get

$$W_e = \frac{1}{8\pi} (\varepsilon_{11} E_1{}^2 + \varepsilon_{22} E_2{}^2 + \varepsilon_{33} E_3{}^2 + 2\varepsilon_{23} E_2 E_3 + 2\varepsilon_{13} E_1 E_3 + 2\varepsilon_{12} E_1 E_2)$$

$$\tag{2.18}$$

To eliminate the last three terms, we rotate the coordinate axes by a suitable angle,

giving

$$W_e = \frac{1}{8\pi} \left(\varepsilon_x E_x{}^2 + \varepsilon_y E_y{}^2 + \varepsilon_z E_z{}^2 \right) \tag{2.19}$$

where x,y,z are the new or principle dielectric axes.

Thus, the dielectric constant can now be given by

$$\begin{vmatrix} D_x \\ D_y \\ D_z \end{vmatrix} = \begin{vmatrix} \varepsilon_x & 0 & 0 \\ 0 & \varepsilon_y & 0 \\ 0 & 0 & \varepsilon_z \end{vmatrix} \begin{vmatrix} E_x \\ E_y \\ E_z \end{vmatrix} \tag{2.20}$$

Also the propagation constant for a crystal is a vector, more commonly known as the

wave vector or the k vector.

$$k = \frac{\omega n}{c} s$$

where s is the unit vector normal to the wavefront. Let us try to examine the

transmission of a monochromatic plane wave through an anisotropic crystal. Let ∇ be

replaced by $(i\omega n/c)s$ and $\delta/\delta t$ by $i\omega$ in equation 2.5 and 2.6 for a nonconducting and a

nonmagnetic crystal.

$$H \times s = \frac{1}{n} D \tag{2.21}$$

$$E \times s = -\left(\frac{1}{n}\right) H \tag{2.22}$$

From the above equations we find that D is perpendicular to H and s, and H is

perpendicular to E and s. Hence D and H constitute a transverse pair. Also (E X H)

the Poynting vector is not normal to E. This means that the direction of energy flow and the wave normal are not parallel.

Let us solve the above equations 2.21 and 2.22 to eliminate H

$$(E \times s) \times s = -(\frac{1}{n^2}) D$$

$$s \times (E \times s) = (\frac{1}{n^2}) D$$

$$E(s \cdot s) - s(s \cdot E) = (\frac{1}{n^2}) D$$

$$D = n^2 (E - s(s \cdot E))$$

In terms of components of D we get

$$D_x = n^2 (\frac{D_x}{\varepsilon_x} - s_x(s \cdot E))$$

$$D_x = \frac{s_x(s \cdot E)}{\frac{1}{\varepsilon_x} - \frac{1}{n^2}} \tag{2.23}$$

Since we know that D and S are perpendicular, taking a scalar product of D, S we get

$$\frac{s_x^2}{\frac{1}{n^2} - \frac{1}{\varepsilon_x}} + \frac{s_y^2}{\frac{1}{n^2} - \frac{1}{\varepsilon_y}} + \frac{s_z^2}{\frac{1}{n^2} - \frac{1}{\varepsilon_z}} = 0 \tag{2.24}$$

This is the Fresnel's equation [4, 26].

It is quadratic in n, having solutions as $\pm n'$, $\pm n''$.

Thus the two corresponding values are D' and D" which can be proved to be orthogonal. Thus, we can conclude that an anisotropic media can transmit waves polarized only in two mutually orthogonal directions with different refractive indices seen in those two directions.

If the incident light is not polarized in either of the allowed directions, then this light will be decomposed into two linearly polarized components in each allowable direction. Both the components see different refractive indices resulting in an output which is not linearly polarized after transmission through the crystal.

2.3 The Index Ellipsoid

To find the allowed directions and the refractive indices for any arbitrary direction of propagation we follow the given procedure.

On rearranging equation 2.19 we get

$$8\pi W_e = \frac{D_1^2}{\varepsilon_1} + \frac{D_2^2}{\varepsilon_2} + \frac{D_3^2}{\varepsilon_3}$$

Let

$$\left(\frac{D_1}{\sqrt{8\pi W_e}}\right) = x$$

and so on gives

$$\frac{x^2}{\varepsilon_1} + \frac{y^2}{\varepsilon_2} + \frac{z^2}{\varepsilon_3} = 1$$

But

$$n = \sqrt{\varepsilon}$$

Hence

$$\frac{x^2}{n_1^2} + \frac{y^2}{n_2^2} + \frac{z^2}{n_3^2} = 1 \tag{2.25}$$

The above equation represents an ellipsoid with the major axis in the x, y, and z directions. It is known as the index ellipsoid or the optical indicatrix. It is used to find the two allowed directions of polarization and the refractive indices in those directions. If the wave normal is considered as the direction of propagation then through the center of the ellipsoid a plane is drawn perpendicular to it. Now this intersection will give us a two directional ellipse. The two axes of this ellipse will give the two allowable polarization and the corresponding refractive indices are equal to half the length of the axis.

There are basically two types of optically anisotropic crystals. If all the three axes of the indicatrix are unequal then the crystal is called Biaxial. It has two different optical axes. If two of the three axes of the indicatrix are equal, then the crystal is defined to be Uniaxial. It has only one optical axis which is perpendicular to the plane of the two equal axes. Now we can define the optic axis as that direction of the wave normal in which the refractive index is independent of the direction of polarization.

For a biaxial crystal with $n_z > n_y > n_x$, the angle θ between the optic axis (either of the two) and the z axis is given by

$$\sin\theta = \frac{n_z}{n_y}\sqrt{(n_y^2-n_x^2)/(n_z^2-n_x^2)} \qquad (2.26)$$

In most of the cases, the crystal is isotropic or anisotropic is determined by the crystal symmetry.

For an anisotropic material Snell's law for refraction is still valid, but with a minor modification.

For o-ray : sin i = n sin r

For e-ray: sin i = n(r) sin r

Also if θ is the angle between the wave normal and the optic axis and ρ is the angle between the ray direction and the optic axis, then we have

$$\tan\rho = (\frac{n_o}{n_e})^2\tan\theta \qquad (2.27)$$

2.4 Birefringence

In the case of uniaxial crystals, the indicatrix is an ellipsoid of revolution. There are two basic allowable directions of polarization. viz. ordinary direction and the extraordinary direction. For the ordinary direction, the refractive index can be plotted by a circle, since it is independent of the direction of propagation. While for the extraordinary direction the plot for the refractive index would look like an ellipse. It has a range of n_o and n_e. It has the value of the ordinary index n_o when it is parallel to the optic axis and varies elliptically to n_e, the value for extraordinary index when it is perpendicular to the optic axis. The beams of light thus produced are known as o-ray

and e-ray respectively. When the wave normal is at an angle θ to the optic axis, its extraordinary index is given by

$$n(\theta) = \frac{n_e n_o}{(n_o^2 \sin^2\theta + n_e^2 \cos^2\theta)} \tag{2.28}$$

When n_e is larger than n_o, the birefringence and hence the corresponding crystal is called positive, and if n_e is smaller than n_o then the birefringence as well as the crystal are called negative uniaxial.

An important application of birefringence is to make two waves with different frequencies to travel with the same velocity inside the crystal by making one of them as an o-ray and the other as e-ray. This phenomenon is used to compensate the color dispersion of a material by birefringence. Another major application is for components that change the state of polarization of a light beam. It is used to create half-wave plates to rotate the polarization direction of a plane-polarized beam over any desired angle, or a quarter wave plate to produce circularly or elliptically polarized light. The quarter-wave plate can also work as an isolator for the incident beam linearly polarized at 45° to its axis, with certain component isolation.

2.5 Optical Activity

In most of the substances, the light travelling parallel to the optic axis would propagate without change in polarization. But there are always exceptions. The phenomenon in which the polarization of the light is rotated inside a crystal is known as optical activity. The amount of rotation of light depends on the wavelength. Quartz

is a good example of this kind. The crystals that show natural optical activity indicate that direction of polarization rotation is independent of the direction of light propagation through the crystal.

2.6 Electrooptic Effect

Anisotropy can be induced in an isotropic material by an outside influence such as strain or an electric field. The outside influence has to be large enough to make the atoms of the medium see different electric field in different directions to have this phenomenon of induced anisotropy to occur. This phenomenon produces a differential change of the refractive indices for two orthogonally polarized beams. This effect could be used to switch the polarization of a light beam using electric field, or to modulate a beam of light.

Let us consider the first-order electrooptic effect in anisotropic crystals. The dielectric constant is a second-rank tensor. The electrooptic coefficient gives the change in the dielectric constant as a result of the applied field. The electrooptic coefficient r_{ij} is a tensor of third rank, which when multiplied by a vector gives a tensor of second rank. The second rank tensor on which this third rank tensor operates is symmetrical, hence there are at the most only 18 independent elements. Most of these 18 elements are zero for cases in which the crystal transforms into itself. In the case of centrosymmetric crystals, all the components are zero, giving no first-order electrooptic effect.

Let $b_{ij} = 1 / n_{ij}^2$ and further more $b_i = i / n_i^2$

then the change of b_i as a result of an applied field can be written as

$$\Delta b_i = r_{ij} E_{R_j}$$

where i runs from 1 to 6 and j from 1 to 3. Thus the electrooptic tensor can be represented by a matrix with 6 rows and 3 columns.

The electrooptic effect produces a change in the index, hence the changed indices if to be presented by an indicatrix, would have a few off-diagonal terms which were not present in the original indicatrix. This phenomenon is used to design electrooptic shutters or modulators.

CHAPTER III

NONLINEAR OPTICS

3.1 Introduction

We know from different areas of physics that the linear dependence of one physical quantity on another is almost always an approximation, with a validity in a limited range only. The refractive index of a material results from the polarization of that material by the electric field of the transmitted radiation. But this polarization would be linear for a limited range of electric field strengths only.

The second harmonic generation experiment of Franken et. al. marked the birth of the field of nonlinear optics [18, 26]. They propagated a ruby laser beam at 6942°A through a quartz crystal and observed ultraviolet radiation from the crystal at 3471°A. Second- harmonic generation is the first nonlinear optical effect ever observed in which a coherent input generates a coherent output. Nonlinear optics deals in general with nonlinear interaction of light with matter and includes such problems as light-induced changes of the optical properties of a medium. Optical pumping was also well known phenomenon in the early days. The resonant excitation of optical pumping includes a redistribution of populations and changes the properties of the medium. Because of resonant enhancement, even a weak light is sufficient to perturb the

material system strongly to make the effect easily detectable. Each nonlinear optical process may consist of two parts. The intense light first induces a nonlinear response in a medium and then the medium in reacting modifies the optical fields in a nonlinear way.

Consider an alternating field instead of a temporally uniform field to analyse the nonlinear effect. The refractive index if modulated by such an alternating field of frequency ω_2 then the field ω_1 passing through this crystal will be phase modulated. As a result the sidebands would be generated giving the sum and the difference frequencies. These phenomena introduce the concept of parametric frequency conversion. This alternating field of frequency ω_2 also modulates the refractive index giving rise to a harmonic overtone at ω_2 and one at $2\omega_1$, for frequency ω_1. But this sideband at $2\omega_1$ is observable only if the beam at ω_1 is very intense. But in the case of sum frequency $(\omega_1 + \omega_2)$ or a difference frequency $(\omega_2 - \omega_1)$ it does not matter if ω_2 is very intense. The detection of a weak signal, at a wavelength for which sensitive detectors dose not exist, is done using this concept.

Nonlinear effects are quite common in microwaves too. The only significant difference between the microwave effect and the nonlinear optics is that the interaction takes place in the bulk in the later part.

3.2 The Anharmonic Oscillator Model

In this model, a medium is composed of a set of N classical anharmonic oscillators per unit volume. The oscillator describes physically an electron bound to a

core of an infrared-active molecular vibration. Its equation of motion in the presence of a driving force is

$$\frac{d^2r}{dt^2} + 2\gamma \frac{dr}{dt} + \omega_o^2 r - \xi r^2 = -\frac{e}{m}E \tag{3.1}$$

Here the anharmonic term is introduced in the Lorentz model, because of which this equation becomes complex. Let us assume that this anharmonic term is very small compared to the harmonic one, giving the correspondingly smaller effects. Let the solution be in terms of a power series

$$r = r_1 + r_2 + r_3 + r_4 + \ldots \ldots + r_n \tag{3.2}$$

where

$$r_n = a_n E^n$$

On substituting equation 3.2 in 3.1 and collecting the terms of the same order in E, we get

$$\frac{d^2 r_1}{dt^2} + 2\gamma \frac{dr_1}{dt} + \omega_o^2 r_1 = -\frac{e}{m}E \tag{3.3}$$

$$\frac{d^2 r_2}{dt^2} + 2\gamma \frac{dr_2}{dt} + \omega_o^2 r_2 = \xi r_1^2 \tag{3.4}$$

Thus we find that the term ξr^2 in equation 3.1 causes displacement that is nonlinear in E and this nonlinearity is $r_2 = a_2 E^2$ in the above example. By successive iterations, higher order solutions can also be obtained. In the second order solution, new frequency components of the polarization at $\omega_1 \pm \omega_2$, $2\omega_1$, $2\omega_2$ and 0 appear

through quadratic interaction of the field with the oscillator via the anharmonic term. The oscillating polarization components will radiate and generate new electro-magnetic waves at $\omega_1 \pm \omega_2$, $2\omega_1$ and $2\omega_2$. This readily explains the sum and the difference frequency generation and the second harmonic generation. A zero frequency polarization term known as optical rectification appears. In general, the frequency components at $\omega = n_1 \omega_1 \pm n_2 \omega_2$, with n_1 and n_2 being the integers, are expected in the higher order terms. The anharmonicity ξ determines the strength of the nonlinear interaction in the anharmonic oscillator model.

3.3 The Nonlinear Polarization

It seems an easier and more convenient approach to consider the interaction as a result of the nonlinearity of polarization, rather than a modulation of the refractive index. The polarization with nonlinear terms is given by

$$P = \alpha E (1 + a_1 E + a_2 E^2 + a_3 E^3 + \cdots\cdots)$$

where α is the linear probability and a_1, a_2, a_3, ... are the nonlinearities of the increasing order. For the center of symmetry $a_1 = a_2 = ...$ have to be equal to zero. For the first nonlinearity,

$$P = 2 d E_R^2 \qquad (3.5)$$

where P is the nonlinear polarization due to the first nonlinearity. Consider the following two waves for interaction within a crystal, neglecting their phases,

$$E_{R_1}(z, t) = E_{R_1} \cos(\omega_1 t + k_1 z)$$

$$E_{R_2}(z, t) = E_{R_2} \cos(\omega_2 t + k_2 z)$$

On substituting the superimposition of the above waves in equation 3.5 we get

$$P = 2d(E_{R_1}(z, t) + E_{R_2}(z, t))^2$$

$$P = 2d(E_{R_1}{}^2 \cos^2(\omega_1 t + k_1 z) + E_{R_2}{}^2 \cos^2(\omega_2 t + k_2 z)$$

$$+ 2E_{R_1}E_{R_2}\cos(\omega_1 t + k_1 z)\cos(\omega_2 t + k_2 z))$$

$$\therefore P = 2d(E_{R_1}{}^2(1 - \cos 2(\omega_1 t + k_1 z))/2) + 2d(E_{R_2}{}^2(1 - \cos 2(\omega_2 t + k_2 z))/2)$$

$$+ 2d((2E_{R_1}E_{R_2})((\cos((\omega_1 + \omega_2)t + (k_1 + k_2)z)/2$$

$$+ (\cos((\omega_1 - \omega_2)t + (k_1 - k_2)z)/2))$$

Thus, we get

$$P = d(E_{R_1}{}^2 + E_{R_2}{}^2) - dE_{R_1}{}^2 \cos(2(\omega_1 t + k_1 z)) - dE_{R_2}{}^2 \cos(2(\omega_2 t + k_2 z))$$

$$+ 2dE_{R_1}E_{R_2}\cos((\omega_1 + \omega_2)t + (k_1 + k_2)z) + 2dE_{R_1}E_{R_2}\cos((\omega_1 - \omega_2)t + (k_1 - k_2)z)$$

Thus, the above polarization consists of a number of components with different

frequencies, and a steady term. They are:

$$P_{2\omega_1} = dE_{R_1}{}^2 \cos(2(\omega_1 t + k_1 z))$$

$$P_{2\omega_2} = dE_{R_2}{}^2 \cos(2(\omega_2 t + k_2 z))$$

$$P_{\omega_1+\omega_2}=2\,dE_{R_1}E_{R_2}\cos\left(\left(\omega_1+\omega_2\right)t+\left(k_1+k_2\right)z\right)$$

$$P_{\omega_1-\omega_2}=2\,dE_{R_1}E_{R_2}\cos\left(\left(\omega_1-\omega_2\right)t+\left(k_1-k_2\right)z\right)$$

and

$$P_{direct}=d\left(E_{R_1}{}^2+E_{R_2}{}^2\right) \tag{3.6}$$

The nonlinear polarization contains a steady term, a sum and a difference

frequency and the first overtone of both the input frequencies, more commonly known

as the second harmonics. These different components generate electromagnetic waves

of frequencies different than that of the incident radiation. Due to this effect, a fraction

of the incident energy used to create the nonlinear polarization can be reemitted at one

or more number of different frequencies. The frequencies that would eventually

dominate at the output of the crystal would depend on the relative phases of the two

different waves of different frequencies at any point in the nonlinear medium. And the

electromagnetic wave radiated by the dipole at this point will have a propagation

velocity that is dependent on the frequency of this resultant wave and the

corresponding refractive index of the material for this frequency. Now, this

propagation velocity of the resultant wave emitted by this sample is completely

different from the propagation velocity of the polarization wave, thus resulting in a

destructive interface. Thus, the entire system of the radiating dipoles does not

necessarily form a correctly phased array of antennas as it did in the linear case, hence

arises a need for the phase matching. This technique is very critical in the case of

nonlinear phenomena and requires a precise control of the indices at the three frequencies involved in the mixing process to match the different propagation velocities.

To examine the interaction of different fields having different frequencies we define the electric field as follows:

$$E = E(\omega_1) e^{-i\omega_1 t} + E^*(\omega_1) e^{i\omega_1 t} + E(\omega_2) e^{-i\omega_2 t} + E^*(\omega_2) e^{i\omega_2 t} + \ldots\ldots$$

$$\ldots\ldots\ldots + E^*(\omega_n) e^{-i\omega_n t} \qquad (3.7)$$

Let $E^*(\omega_n) = E(\omega_{-n}) = E(-\omega_n)$

Thus, we get

$$E = \sum_n E(\omega_n) e^{-i\omega_n t} \qquad (3.8)$$

where n is an integer.

Let us try to derive the nonlinear polarization using the equations obtained from the anharmonic oscillator model.

$$r_1 = a_1 E$$

$$r_1 = a_1 \sum_n E(\omega_n) e^{-i\omega_n t}$$

$$\therefore \quad \frac{dr_1}{dt} = -i a_1 \sum_n E(\omega_n) e^{-i\omega_n t} \cdot \omega_n$$

$$\therefore \quad \frac{d^2 r_1}{dt^2} = -a_1 \sum_n E(\omega_n) \, e^{-i\omega_n t} \cdot \omega_n^2$$

On substituting in equation 3.3 we get

$$a_1 \sum_n E(\omega_n) \, e^{-i\omega_n t} \cdot \omega_n^2 - 2 a_1 i\gamma \sum_n E(\omega_n) \, e^{-i\omega_n t} \cdot \omega_n + a_1 \omega_0^2 \sum_n E(\omega_n) \, e^{-i\omega_n t}$$

$$= -\frac{e}{m} \sum_n E(\omega_n) \, e^{-i\omega_n} \tag{3.9}$$

on equating the terms with the same frequencies on both sides,

$$a_1 \sum_n E(\omega_n) \, e^{-i\omega_n t} = -\frac{e}{m} \sum_n \frac{E(\omega_n) \, e^{-i\omega_n t}}{(\omega_0^2 - 2i\gamma\omega_n - \omega_n^2)}$$

$$r_1 = -\frac{e}{m} \sum_n \frac{E(\omega_n) \, e^{-i\omega_n t}}{(\omega_0^2 - 2i\gamma\omega_n - \omega_n^2)} \tag{3.10}$$

The above equation is used to find terms of next higher order.

Using equations 3.4 and 3.10 we get

$$r_2 = -\frac{e^2 \xi}{m^2} \sum_n \sum_m \frac{E(\omega_n) E(\omega_m) \, e^{-i(\omega_n \omega_m) t}}{F(\omega_0, \omega_n, \omega_m, \xi)} \tag{3.11}$$

where

$$F(\omega_0, \omega_n, \omega_m, \gamma) = (\omega_n^2 - 2i\omega_n\gamma - \omega_n^2)(\omega_0^2 - 2i\omega_m\gamma - \omega_m^2)$$

$$\times (\omega_0^2 - 2i(\omega_n + \omega_m)\gamma - (\omega_n + \omega_m)^2)$$

Similarly, for the polarization density, we write a power series,

$$P = \sum_{i=1}^{\infty} P_e$$

where

$$P_e = -Ner_e$$

Thus, the linear polarization is given by

$$P_{linear} = \sum \chi^{(1)}(\omega_n) E(\omega_n) e^{-i\omega_n t}$$

where

$$\chi^{(1)}(\omega_n) = \frac{Ne^2}{m} \frac{1}{\omega_0^2 - 2i\gamma\omega_n - \omega_n^2}$$

and for the second order polarization

$$P_{second} = \sum_n \sum_m \chi^{(2)}(\omega_n, \omega_m) E(\omega_n) E(\omega_m) e^{-i(\omega_n + \omega_m)} \qquad (3.12)$$

where

$$\chi^{(2)}(\omega_n, \omega_m) = -\frac{m\xi}{N^2 e^3} (\chi^{(1)}(\omega_n)) (\chi^{(1)}(\omega_m)) (\chi^{(1)}(\omega_n + \omega_m))$$

$$(3.13)$$

The second order polarization obtained above is due to the nonlinear term ξr^2 in equation 3.1. If a third or higher order terms would have been included in that equation, then the third or the higher order polarization would have been obtained.

Another important thing observed over here is that the higher order susceptibilities always depend on the lower order susceptibilities. The number of

independent components in equation 3.13 can be further reduced if this idea is applied

to a three dimensional concept. The modified equation 3.12 in a three dimensional

form can be written as

$$P_i(\omega_{n+m}) = \sum_{jk} \sum_{nm} \chi_{ijk}(\omega_{n+m}, \omega_n, \omega_m) E_j(\omega_n) E_k(\omega_m) e^{-i(\omega_n+\omega_m)t} \quad (3.14)$$

where i, j, k each take values x, y and z.

Let us consider only the nonlinear terms involved in the sum-frequency

generation for the interaction of $E(\omega_{n+m})$ with $E(\omega_n)$ and $E(\omega_m)$. These terms are

$$
\begin{aligned}
P_i(\omega_1) &= \chi_{ijk}(\omega_1, -\omega_2, \omega_3)\; E_j(-\omega_2) E_k(-\omega_3)\, e^{-i(\omega_3-\omega_2)t} \\
&+ \chi_{ijk}(\omega_1, \omega_3, -\omega_2)\; E_j(\omega_3) E_k(-\omega_2)\, e^{-i(\omega_3-\omega_2)t}
\end{aligned}
$$

$$
\begin{aligned}
P_j(\omega_2) &= \chi_{jki}(\omega_2, \omega_3, -\omega_1)\; E_k(\omega_3) E_i(-\omega_1)\, e^{-i(\omega_3-\omega_1)t} \\
&+ \chi_{jki}(\omega_2, -\omega_1, \omega_3)\; E_k(-\omega_1) E_i(\omega_3)\, e^{-i(\omega_3-\omega_1)t}
\end{aligned}
$$

$$
\begin{aligned}
P_k(\omega_3) &= \chi_{kij}(\omega_3, \omega_1, \omega_2)\; E_i(\omega_1) E_j(\omega_2)\, e^{-i(\omega_1+\omega_2)t} \\
&+ \chi_{kij}(\omega_3, \omega_2, \omega_1)\; E_j(\omega_1) E_i(\omega_2)\, e^{-i(\omega_1+\omega_2)t}
\end{aligned} \quad (3.15)
$$

and three more terms for the negative frequencies. Now, since the first order

susceptibility is real, we get

$$\chi_{ijk}(\omega_1, -\omega_2, \omega_3) = \chi_{jki}(\omega_2, \omega_3, -\omega_1) = \chi_{kij}(\omega_3, \omega_1, \omega_2) \quad (3.16)$$

Thus, the frequencies can be easily permuted, reducing the number of

independent components to 27.

It is not physically possible to decide during the interaction of two waves

which one arrived first. Hence a column vector F is usually introduced as a

mathematical convenience to make sure that the sequence of the two interacting fields

would not be important. This further reduces the number of independent components

to 18, since $d_{ijk} = d_{ikj}$.

In the case of optical rectification, where a wave interacts with itself, the end

result is only a phase change in the transmitted wave. This apparently changes the

refractive index of the crystal, giving the electrooptic effect. Thus it could be

concluded that the coefficients of the optical refraction are same as those for the

electrooptic effect, with a proper interchange of the indices.

3.4 Miller's Rule

Miller defined a coefficient [26]

$$\Delta_{ijk} = \frac{\chi_{ijk}^{(2)}(\omega_3 = \omega_1 + \omega_2)}{\chi_{ii}^{(1)}(\omega_3)\,\chi_{jj}^{(1)}(\omega_1)\,\chi_{kk}^{(1)}(\omega_2)} \qquad (3.17)$$

The above coefficient which matches the relation obtained in the equation 3.13

when generalized to three dimensions, is known as the Miller's coefficient, and the

relation is famous as the Miller's Rule. He found empirically that Δ_{ijk} has only weak

dispersion and is almost a constant for a wide range of crystals. This rule is widely

used for the search of new materials. It suggests that high refractory materials should

have large nonlinear susceptibilities. The weak dispersion of Δ_{ijk} can be seen from

either the bond-charge or the charge-transfer model. This Miller's coefficient is

independent of frequencies. The values of Δ_{ijk} for most nonlinear crystals are around

few times 10^{-6}esu [26].

To avoid any confusion about the relationship between the nonlinear

susceptibility Δ and the more practically used nonlinear coefficient d, the following

relation is used for this thesis.

$$d = \frac{1}{2}\chi(2\omega_1, \omega_1, \omega_1)$$

Assuming all frequencies to lie within the optical transmission region of the

crystal, we can set the susceptibilities equal, thus getting a generalization in three

dimensions as

$$d_{ijk} = \frac{1}{2}\chi_{ijk}$$

3.5 Crystal Symmetry

The crystals that have a center of symmetry cannot exhibit a second-order

polarization. The crystals are divided into 32 different classes, out of which there is

only one class viz. class 1 in triclinic system, which does not have centro-symmetry.

For all the other classes, performing the symmetry operations which transform the

crystal into itself on the susceptibility matrix, no change is found in the matrix.

3.6 The Coupled Amplitude Equations

To derive the equations for the electromagnetic radiation generated by the

nonlinear polarization let us consider three interacting waves and than seek three

coupled amplitude equations, each giving the rate of growth, or decay of the field at

one frequency as a function of the fields at the two other frequencies.

The nonlinear polarization is introduced in Maxwell's equations as a source term as follows:

$$\nabla \times H = \frac{1}{c} \frac{\partial D}{\partial t} \tag{3.18}$$

$$\nabla \times E = -\frac{1}{c} \frac{\partial}{\partial t} (\mu H) \tag{3.19}$$

$$D = \varepsilon E + 4\pi P$$

Again the linear polarization is included in ε and P is only the nonlinear polarization, as done previously.

The material is assumed to be nonconducting and nonmagnetic. Taking curl on both the sides of equation 3.19 and putting $\nabla \cdot E = 0$, we get

$$\nabla^2 E = \frac{\partial^2}{\partial t^2} (\frac{\varepsilon}{c^2} E) - \frac{4\pi}{c^2} \frac{\partial^2 P}{\partial^2} \tag{3.20}$$

For a single dimension restricted problem $\delta/\delta y = 0$ and $\delta/\delta x = 0$

Let the three interacting traveling waves be defined as:

$$E_1(z, t) = E_1(z) e^{-i(\omega_1 t - k_1 z)}$$

$$E_2(z, t) = E_2(z) e^{-i(\omega_2 t - k_2 z)}$$

$$E_3(z, t) = E_3(z) e^{-i(\omega_3 t - k_3 z)} \tag{3.21}$$

In the nonlinear case, the complex amplitude changes as a result of interaction with waves at different frequencies. The z dependence of the phase Φ is shown as

$$E_1(z) = \frac{1}{2} E_{R_1}(z) e^{i\phi(z)}$$

We rewrite the nonlinear polarization components of equation 3.15 as

$$P_1(z, t) = 4dE_2^*(z) E_3(z) e^{-i((\omega_3-\omega_2)t-(k_3-k_2)z)}$$

$$P_2(z, t) = 4dE_3(z) E_1^*(z) e^{-i((\omega_3-\omega_1)t-(k_3-k_1)z)}$$

$$P_3(z, t) = 4dE_1(z) E_2(z) e^{-i((\omega_1+\omega_2)t-(k_1+k_2)z)} \tag{3.22}$$

Thus, the z dependence is clearly indicated in the above equations.

The restricted equation 3.20 can be rewritten with the substitution of the following results.

$$\frac{\partial P_1}{\partial t} = 4dE_2^*(z) E_3(z) e^{-i((\omega_3-\omega_2)t-(k_3-k_2)z)} \cdot (\omega_3-\omega_2)(-i)$$

$$\frac{\partial^2 P_1}{\partial t} = (\omega_3-\omega_2)^2 4dE_2^*(z) E_3(z) e^{-i((\omega_3-\omega_2)t-(k_3-k_2)z)}$$

$$\frac{\partial^2 P_2}{\partial t} = (\omega_3-\omega_1)^2 4dE_3(z) E_1^*(z) e^{-i((\omega_3-\omega_1)t-(k_3-k_1)z)}$$

$$\frac{\partial^2 P_3}{\partial t} = (\omega_1+\omega_2)^2 4dE_1(z) E_2(z) e^{-i((\omega_1+\omega_2)t-(k_1+k_2)z)}$$

and

$$\frac{\partial E_1(z, t)}{\partial t} = E_1(z) e^{-i(\omega_1 t-k_1 z)} k_1(i) + \frac{\partial E_1(z)}{\partial z} e^{-i(\omega_1 t-k_1 z)}$$

$$\therefore \frac{\partial E_1(z,t)}{\partial t} = (ik_1 E_1(z) + \frac{\partial E_1(z)}{\partial z}) e^{-i(\omega_1 t - k_1 z)}$$

$$\therefore \frac{\partial^2 E_1(z,t)}{\partial t} = (ik_1 \frac{\partial E_1(z)}{\partial z} + \frac{\partial^2 E_1(z)}{\partial z^2}) e^{-i(\omega_1 t - k_1 z)}$$
$$+ (ik_1 E_1(z) + \frac{\partial E_1(z)}{\partial z}) (k_1 i) e^{-i(\omega_1 t - k_1 z)}$$

$$\therefore \frac{\partial^2 E_1(z,t)}{\partial t} = (ik_1 \frac{\partial E_1(z)}{\partial z} + \frac{\partial^2 E_1(z)}{\partial z^2}) - k_1^2 E_1(z) + ik_1 \frac{\partial E_1(z)}{\partial z}) e^{-i(\omega_1 t - k_1 z)}$$

Hence,

$$\frac{\partial^2 E_1(z,t)}{\partial t} = -(k_1^2 E_1(z) - 2ik_1 \frac{\partial E_1(z)}{\partial z} - \frac{\partial^2 E_1(z)}{\partial z^2}) e^{-i(\omega_1 t - k_1 z)}$$

Since the variation of the complex field amplitude with z is very small,

$$\frac{\partial^2 E_1(z,t)}{\partial z^2} << \frac{\partial E_1(z)}{\partial z} \times k$$

$$\therefore \frac{\partial^2 E_1(z,t)}{\partial t} = -(k_1^2 E_1(z) - 2ik_1 \frac{\partial E_1(z)}{\partial z}) e^{-i(\omega_1 t - k_1 z)}$$

$$\therefore \frac{\partial^2 E_2(z,t)}{\partial t} = -(k_2^2 E_2(z) - 2ik_2 \frac{\partial E_2(z)}{\partial z}) e^{-i(\omega_2 t - k_2 z)}$$

and

$$\therefore \frac{\partial^2 E_3(z,t)}{\partial t} = -(k_3^2 E_3(z) - 2ik_3 \frac{\partial E_3(z)}{\partial z}) e^{-i(\omega_3 t - k_3 z)}$$

with $\varepsilon \omega^2 / c = k^2$

Thus, we now write equation 3.20 for each frequency component as

$$\frac{dE_1(z)}{dz} = -i\frac{8\pi\omega_1^2}{k_1c^2}dE_2^*(z)\,E_3(z)\,e^{i(k_3-k_2-k_1)z}$$

$$\frac{dE_2(z)}{dz} = -i\frac{8\pi\omega_2^2}{k_2c^2}dE_1^*(z)\,E_3(z)\,e^{i(k_3-k_2-k_1)z}$$

$$\frac{dE_3(z)}{dz} = -i\frac{8\pi\omega_3^2}{k_3c^2}dE_1E_2(z)\,e^{i(k_1+k_2+k_3)z} \qquad (3.23)$$

These three equations are known as the coupled amplitude equations. All the three amplitude depend on each other as the name suggests.

Let $\Delta k = k_3 - k_2 - k_1$

The problem becomes much easier when we assume that the input amplitude remains nearly constant. For such a simplified case, we obtain the following set of results through basic substitutions.

$$E_3 = -\frac{8\pi\omega_3^2}{k_3c^2\Delta k}dE_1E_2\,(e^{i\Delta kL}-1) \qquad (3.24)$$

where L is the length of the crystal.

For $\omega = 2\pi c/\lambda$ and $k = 2\pi n/\lambda_3$

$$E_3 = -\frac{16\pi^2}{n_3\lambda_3\Delta k}dE_1E_2\,(e^{i\Delta kL}-1) \qquad (3.25)$$

The power per unit area in a material is given by

$$S = \frac{cn}{8\pi}E_R^2$$

$$S = \frac{cn}{8\pi} EE^*$$

$$S_3 = \frac{512\pi^2 L^2 d^2 W_1 W_2}{n_1 n_2 n_3 \lambda_3^2 c} \left(\frac{\sin x}{x}\right)^2 \tag{3.26}$$

where n is the index of the material

and $x = \Delta kL/2$

The Total power W for an area A is given by

$$W_3 = \frac{512\pi^2 L^2 d^2 W_1 W_2}{n_1 n_2 n_3 \lambda_3^2 c} \left(\frac{\sin x}{x}\right)^2 \tag{3.27}$$

The following deductions can be made from equations 3.26. If $\Delta k = 0$, then the power generated is proportional to the square of the length of the crystal, otherwise it varies as $(\sin x/x)^2$. The most important point to be noted is that the output power (in low conversion limits) is proportional to the product of the input power. This is used to check whether the observed signal is actually the derived output signal or not. If the input signal's power is reduced then the output power has to decrease by double the amount, to be the actual signal and not any scattered fraction of the input. Even the factor 'd' helps to check the mixed frequency nature of the observed output.

3.7 The Manley-Rowe Relations

The Manley-Rowe relations were initially derived for lossless nonlinear electronic circuit elements. They were later generalized to include nonlinear continuous media. Let us consider the three coupled amplitude equations to obtain this relation. We find that for a perfect phase matching or $\Delta k = 0$, the output power of the sum-

frequency generation in a nonabsorbing bulk medium in low conversion limit is
proportional to L^2 the square of the length of the medium. When L is increased
infinitely, then the output power should also become infinite, which cannot be true.
This happens because at higher value of L, the output power becomes comparable to
the pump or source power. This violates the basic assumption of negligible pump
power depletion. To get a complete solution we go through the following procedure.
The modified equations for $\Delta k = 0$ are

$$\frac{n_1 c}{\omega_1} E_1^* \frac{dE_1}{dz} = -8\pi i d E_1^* E_2^* E_3 \tag{3.28}$$

$$\frac{n_2 c}{\omega_2} E_2^* \frac{dE_2}{dz} = -8\pi i d E_2^* E_1^* E_3 \tag{3.29}$$

$$\frac{n_3 c}{\omega_3} E_3^* \frac{dE_3}{dz} = -8\pi i d E_3^* E_2 E_1 \tag{3.30}$$

The input fields E_1 and E_2 could be interchanged to obtain the first coupled
equation from the other or vise versa. But this is not true for the third equation. This is
reflected in the above modified equations. The right-hand sides of equations 3.28 and
3.29 are equal to the complex conjugate of the right-hand side of the equation 3.30.
On equating them and then applying the formula for power unit area, we get the ratio,

$$\frac{change\ in\ power\ at\ \omega_1}{\omega_1} = \frac{change\ in\ power\ at\ \omega_2}{\omega_2}$$
$$= -\frac{change\ in\ power\ at\ \omega_3}{\omega_3}$$

This is the famous Manley-Rowe Relation [18, 25, 26]. We observe that the

total power flow is independent of z. This relation is valid for both up and down conversions. For sum-frequency generation, $\omega_3 = \omega_1 + \omega_2$ according to the above relation, the sum-frequency gains the power which is lost by both the input lasers. But for difference-frequency generation, $\omega_3 - \omega_2 = \omega_1$. We find that the source of frequency at ω_3 losses power not only to the generated frequency but also to the other source at ω_2. In terms of the photon density, we see that one photon at ω_1 and the other at ω_2 combine to give one photon at ω_3.

The concept of difference-frequency generation eventually is used to build a parametric oscillator, implementing the Manley-Rowe relations. In this case the source at ω_2 gains power. Thus, a weak source at ω_2 is made to complete multiple passes in a nonlinear cavity resonant at ω_2 to build up this weak signal.

3.8 Sum-Frequency Generation

Sum-frequency generation is one of the first three nonlinear optical effects discovered in the early days. It has gained the maximum importance in the recent days due to its usefulness in extending the tunable laser range to shorter wavelengths.

The physical interpretation of sum-frequency generation is very simple. The two laser beams at ω_1 and ω_2 interact in a nonlinear crystal and generate nonlinear polarization P. It acts as a source of radiation at $\omega_3 = \omega_1 + \omega_2$, due to the collection of oscillating dipoles. The radiation pattern depends on the phase-related spatial distribution of P. By implementing the phase matching conditions, this radiation has to be peaked in a certain direction. As discussed earlier, the energy at the frequencies ω_1

and ω_2 is converted as the energy for ω_3. The conservation of the momentum leads to the relationship $k_3 = k_1 + k_2$ between the wave vectors at the three frequencies. This point of view also suggests that the number of output photons at ω_3 cannot exceed the input number of photons at ω_1.

3.9 Difference-Frequency Generation

Difference-frequency generation is of great technical importance since it provides a means for generating intense coherent tunable radiation in the infrared. Infrared lasers may seem to have all the desired properties as the infrared sources, but their output frequencies are usually discrete without any tunability. However, using the principles of difference-frequency generation it is possible to achieve this tunability. If the pump intensities are approximated as constants, then the difference-frequency generation nearly follows the sum-frequency generation. It is given by the relation $\omega_3 - \omega_2 = \omega_1$. Here, one of the sources at ω_2 gains power with the generated output. Difference-frequency generation being coherent with high average or peak intensity, finds many applications in field of infrared sciences.

3.10 Second-Harmonic Generation

The second-harmonic generation experiment performed by Franken, Hill, Peters and Weinreich started a new chapter in the field of nonlinear optics [18, 26]. A ruby laser beam at 6942°A was focussed on the front surface of a crystalline quartz plate. The radiation emitted was examined with the spectrometer and it was found that it contained a frequency at twice the input frequency.i.e. at $\lambda = 3471°A$. The conversion

efficiency was about 10^{-8}. But this was eventually improved by using more efficient materials, higher intensity lasers, and index-matching techniques.

This is a special case of frequency mixing, where both the input frequencies are equal. Using the principles of sum-frequency generation, the resultant output turns out to be twice the frequency of the input. This would be derived in detail in chapter V. The amplitude coupled equations for this case could not be derived by simply substituting $\omega_1 = \omega_2$ in the previously derived amplitude coupled equations, as it would give a polarization at 2ω.

This effect has found wide application as a means to extend coherent light sources to shorter wavelengths, or in simple words, this method has set a trend for frequency multiplication.

3.11 Reflections At The Boundary

In the direction of propagation, all the radiating dipoles interfere constructively, while for any other directions there is a destructive interference. This was the case for the continuous media. But at the boundary, according to the Fresnel's reflection law, the radiating dipoles are different at both the sides. Hence there is a backward coherent reflection. For a nonlinear case, where higher harmonics and other mixed frequencies are present in the polarization, the backward reflection may contain these components. They would not have the angle of reflection same as the angle of incidence as it would be true for linear reflected waves only.

CHAPTER IV

PHASE MATCHING IN NONLINEAR CRYSTALS

4.1 Introduction

For a nonlinear case, the output consists of higher harmonic terms along with the mixed frequency components. According to the Lorentz model, there would be a constructive interference of the radiating dipoles in the propagation direction for the linear terms. But for the other terms there would be a destructive interference. The phase would be perfectly matched only for the input frequency. For any other frequency, there would be a phase mismatch. This is caused because of the nonlinear term introduced in the Lorentz model, and as a result, Δk is introduced in the amplitude coupled equations. To eliminate this problem, we try to make $\Delta k = 0$. Another important point that we need to find is that the angle over which the output would be radiated for such a phased array, since the output frequency would be completely different from that of the input. Theoretically it is found that the angular distribution of the output radiation is determined by the Fraunhofer diffraction pattern of an aperture with a radius equal to that of a sample cylinder used for the derivation, multiplied by a term that depends on the phase mismatch due to an angle Φ [26].

40

4.2 Non-Phase-Mismatched Case

The output signal generated by a nonlinear crystal after an input wave

propagates through it is alternating in nature. As thickness of the crystal increases, the

output signal alternatively increases and goes to zero. If $\Delta k = 0$, then the crystal is said

to be phase-matched and in the low conversion limits the power generated is

proportional to the square of the length of the crystal. But if $\Delta k \neq 0$, then it is a non-

matched case. Here, the output signal is fluctuating in nature. The crystal length at

which the signal reaches its first maxima is known as the coherence length. For a

phase-matched case, the highest expectation for an output signal should not exceed the

signal from one coherence length.

As mentioned earlier, for a nonlinear interaction, there are more than one

frequency components generated, and most of them are not phase matched, with the

exception of one or two. The power fed into the crystal is not lost, even though there

is a phase mismatch. This power is coupled from the input wave to the output wave

frequency with a phase match and vise versa.

The variation of second-harmonic signal with crystal length plotted by Turhune

et al. for a quartz crystal is depicted in figure 1 [16].

4.3 Phase-Matching Conditions

Under a normal condition, all optical media are weakly nonlinear. But

noticeable nonlinear effects can be observed only when light propagates through

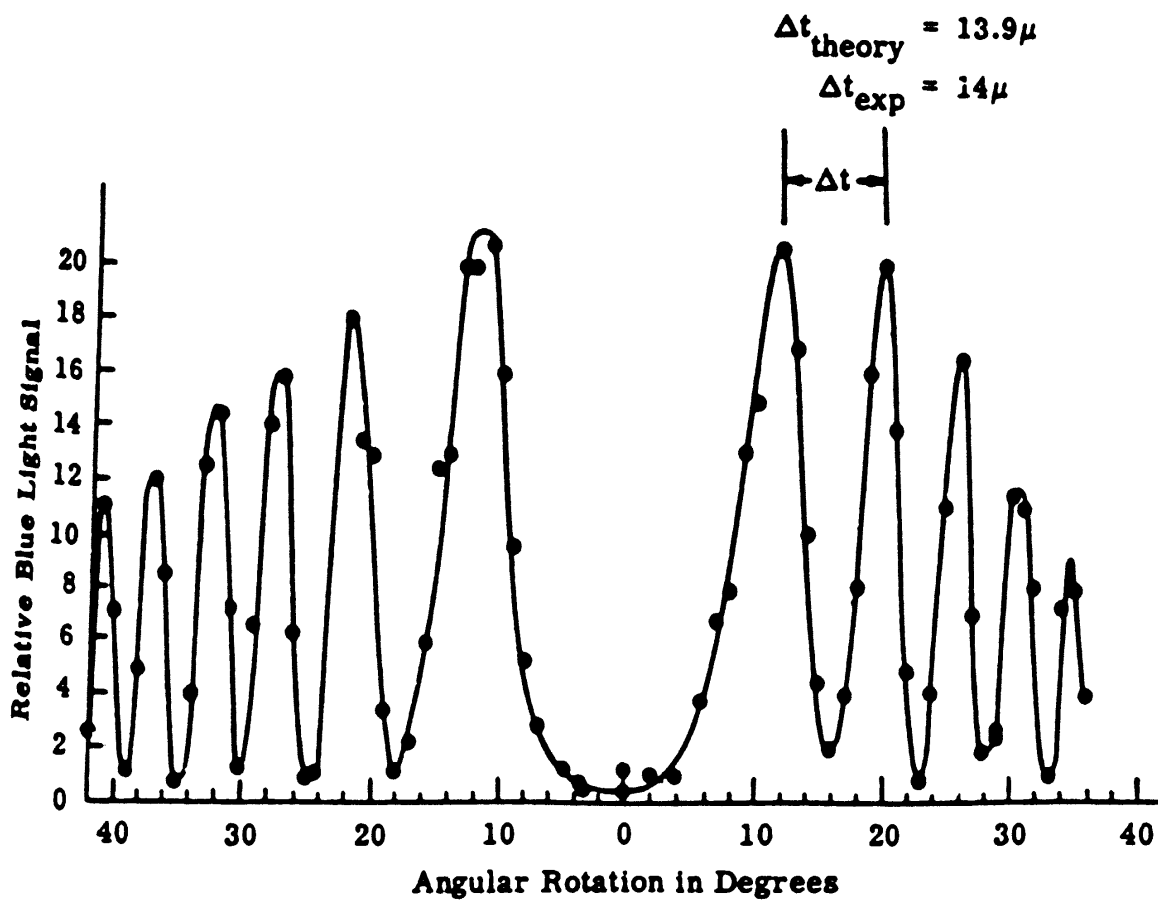comparatively long crystals, with the phase-matching conditions satisfied.

Figure 1. Variation of Second-Harmonic Signal with Crystal Length [16]

i.e. $k_3 = k_2 + k_1$ or $\Delta k = 0$

The relative location of wave vectors under the phase matching can be either collinear or noncollinear.

4.4 Types Of Phase Matching In Uniaxial Crystals

4.4.1 Quasi-Phase Matching Method

The quasi-phase-matched condition is obtained when the phase difference between the polarization wave and the electro-magnetic wave is made equal to $\pi/2$ for every increase of one coherence length of the crystal. But one coherence length will give a signal that is only $4/\pi^2$ times greater than the non-phase-matched signal. Hence it is necessary to put small plates of the crystal having length equal to one coherence length and each adjacent plate turned opposite with a perfect optical contact as suggested by Bloembergen et al [1]. Another method suggested by Bloembergen et al [26]. and experimentally verified by Ashkin et al [2]. and by Boyd and Patel [5] is as follows. It works on the principle of phase change due to total internal reflection within the crystal. The angle of reflection is to be chosen such that the accumulated phase mismatch in every pass between the two reflecting sides is cancelled by the phase change difference between the fundamental and the second-harmonic reflection. This method can be used even for isotropic materials.

4.4.2 Angle Phase Matching

Turhune and co-workers found out a method that employs the birefringence of a uniaxial crystal for a true phase matching. As we know, the index for an extraordinary ray can be varied by changing the angle between the wavenormal and the optic axis. For a positive crystal, the refractive index for the extraordinary ray is higher than that for an ordinary ray. For a collinear phase matching of a second-harmonic generation, we need equal refractive indices for the second-harmonic and the fundamental frequencies. This is obtained by transmitting the wave at an angle θ to the optic axis. For a positive crystal we take the extraordinary rays as fundamentals and the ordinary ray as the second-harmonic, while for the negative crystal it is the other way round. Even a mixing of two different types of rays could produce an extraordinary second harmonic for the negative crystal. This is done for all those wavelengths λ in a negative crystal for which the ordinary index is higher than the extraordinary index at $\lambda/2$, and vise versa for a positive crystal.

If both the fundamental rays have the same polarization, then the sum-frequency radiation would be polarized in the perpendicular direction. In this case a type I phase matching is realized. It could be either "ooe" or "eeo" interaction. If the mixing waves are of orthogonal polarization, type II phase matching takes place. These could be "oee" or "eoe" interactions or "oeo" or "eoo" interactions depending on the type of the crystal.

This method of phase matching has got a few disadvantages. The extraordinary beam does not overlap the ordinary beam in the entire interaction length for

intermediate values of θ other than 0 or 90 degrees. Thus for a type I phase matching it is found that the output is not proportional to the square, but to a lower power of the length. But a more drastic effect results when a type II interaction takes place. Here the polarization wave vanishes completely after a certain crystal length, resulting in no mixing. Another disadvantage is due to the divergence of the focussed beam. Here, the efficient phase matching is achieved for a restricted length of crystal due to linear dependence of Δk with $\Delta \theta$.

4.4.3 Temperature-Dependent Phase Matching

This method was found out to overcome the divergence problem of the previous method. Here, the angle for matching of the indices is suggested to be kept 90 degrees. So that there are no walk-off effects of the first order due to double refraction. This is known as noncritical phase matching, and is done by changing the temperature of the crystal to get $\theta = 90°$. This happens as the extraordinary index is more sensitive to the temperature change. Another method of changing the exact temperature for 90 degrees phase matching is by changing the chemical composition of the crystal.

4.5 Phase Matching In Biaxial Crystals

For biaxial crystals, the refractive indices correspond to a much more complex surface than that for uniaxial crystals. The surface has a bilayer structure with four points of interlayer contact through which two optic axes passes.

Let us consider only one case over here, i.e. $n_x < n_y < n_z$. The angle V_z formed by one of the optic axes with the z axis is given by

$$\sin V_z = \frac{n_z}{n_y} \left(\frac{n_y^2 - n_x^2}{n_z^2 - n_x^2} \right)^{\frac{1}{2}}$$

Let us find out the values of n_0 and n_e for all the three planes viz. XY, YZ and XZ.

For XY plane :

$n_0 = n_z$

and

$$n_e(\phi) = n_y \left(\frac{1 + \tan(\phi)^2}{1 + (n_y/n_x)^2 \tan\phi^2} \right)^{\frac{1}{2}} \qquad ; \quad 0^0 \leq \Phi \leq 90^0$$

For YZ plane :

$n_0 = n_x$

and

$$n_e(\theta) = n_y \left(\frac{1 + \tan(\theta)^2}{1 + (n_y/n_y)^2 \tan\theta^2} \right)^{\frac{1}{2}} \qquad ; \quad 0^0 \leq \theta \leq 90^0$$

For XZ plane :

When $\theta > V_z$ it acts as a positive uniaxial crystal and for $\theta < V_z$ it acts like a negative uniaxial crystal.

The values of n_0 and n_e changes accordingly for $n_x > n_y > n_z$ with V_z given by

$$\cos V_z = \frac{n_x}{n_y} \left(\frac{n_y^2 - n_z^2}{n_x^2 - n_z^2} \right)^{\frac{1}{2}}$$

A detailed table with equations for calculating the phase matching angle upon

collinear propagation of interacting waves in the principal planes of a biaxial crystals could be referred from the book by V.G. Dmitriev et al [7].

4.6 Additional Phase-Matching Methods

Another prominent method used for phase matching utilizes the concept of total internal reflection. There are several other methods employed for phase matching. Some of them have matching in optically active media while a few use the Faraday rotation for matching, or match them acoustically. Recently optical waveguides have been used to reduce the mismatch.

4.7 Nonlinear Materials

As discussed before, the noncentrosymmetricity is a must for any crystal that needs to be qualified for its use in any experiment dealing with three wave mixing. Another requirement for that crystal is its transparency for all the frequencies in the interaction. Quartz satisfied these conditions and was used initially for visible and near-infrared regions. Further experiments revealed that the crystals should be birefringent, and should allow phase matching. The crystals must have excellent optical quality. Hence, the first approach would be to search for best combinations among all the available data on the crystalline materials for refractive index, transmission and crystal class. The crystal growing process was a very determining factor in the successful search of a new nonlinear material. For most of the crystals, the refractive index was very sensitive to the chemical composition of the crystal. And

the crystal growing process may alter the chemical composition of the crystal. Even the crystal composition changes along the length, during the growing process. Thus, the quality of the crystal grown varies from process to process. A perfect crystal would give a plot of second-harmonic power versus temperature as a $(\sin x/x)^2$ function. This has become a standard acceptance test.

4.8 Kurtz Powder Assessment Method

In 1968 S. K. Kurtz described an important new technique for making a quick survey of nonlinear materials [15, 26]. The search for new nonlinear materials became easier, after this technique was found. Before this, it was necessary to grow a crystal to test its nonlinearity. The crystal growing process is a very slow and difficult task. Kurtz found out a technique with which it was possible to find out the nonlinearity of a crystal from the measurement on its powder form. It also indicated whether phase matching is possible for a crystal or not. Thus, the material most ideal for an experiment is first found out by this method, and then it is made to grow into a crystal form. Kurtz surveyed a lots of materials using his method and classified them as either large coefficients, or small coefficient and phase matchable or non-phase matchable and centrosymmetric materials.

CHAPTER V

TYPES OF SECOND-ORDER NONLINEAR OPTICAL PROCESSES

5.1 Introduction

The demonstrations proving higher efficiency of conversion from fundamental to second-harmonic frequencies started the trend of experiments to reach the unattainable wavelengths by using the concept of frequency doubling.

There are two ways of visualizing second-order nonlinear processes. The first view explains this effect as modifying the refractive index of the medium because of the field associated with the first beam. And this results in the modification of the propagation characteristics of the second beam. The first field component could be at some frequency ω_1 and modulate the refractive index at that frequency. A second field passing through the medium at ω_2 would then be phase modulated and exhibit sidebands at the sum and the difference frequencies. If the frequencies ω_1 and ω_2 are identical, then a harmonic overtone at 2ω is created. Thus comes the name parametric processes for them since they result from the modulation of the parameters of the medium.

According to the second view, the nonlinear optical effects result from nonlinearities in the polarization response to incident fields at the various frequencies.

This has been discussed at length in the previous chapters. These second-order nonlinear processes are categorized according to the frequency, intensity and phases of the field components.

Second-harmonic generation is one of the best known and highly utilized effects in nonlinear optics. In this process energy is redistributed between the fields as a result of interaction of the waves with the medium and no energy is lost to the medium, and this is done mainly by conserving the momentum i.e. by phase matching.

When the frequencies ω_1 and ω_2 are not identical, the processes of sum and difference frequency occur. These are schematically shown in figure 2.

In the case of sum frequency generation under phase-matched condition, ω_1 and ω_2 lose power to the sum frequency ω_3. While for difference frequency, the source at ω_3 loses power both to the difference frequency ω_1 and the source at ω_2.

5.2 Second-Harmonic Generation

Let us try to analyze the coupled amplitude equations for phase matched conditions. Here, both the input frequencies are equal, and hence the output frequency is twice the input frequency. But the amplitude coupled equations cannot be obtained simply by substituting $\omega_1 = \omega_2$ in the equations 3.23, as this would give the polarization at 2ω which is not true. Second harmonic has only term $\omega_1 + \omega_1$ (or $\omega_2 + \omega_2$) taken once. The amplitude coupled equations are [26] :

$X_{ijk}^{(2)}(-w_3;w_2,w_1)$

w_2

w_1

w_3

SUM GENERATION

$w_3 = w_2 + w_1$

$X_{ijk}^{(2)}(-w_1;w_3,w_2)$

w_3

w_1

w_2

DIFFERENCE GENERATION

$w_1 = w_3 - w_2$

$X_{ijk}^{(2)}(-w_2;w_3,w_1)$

w_3

w_1

w_2

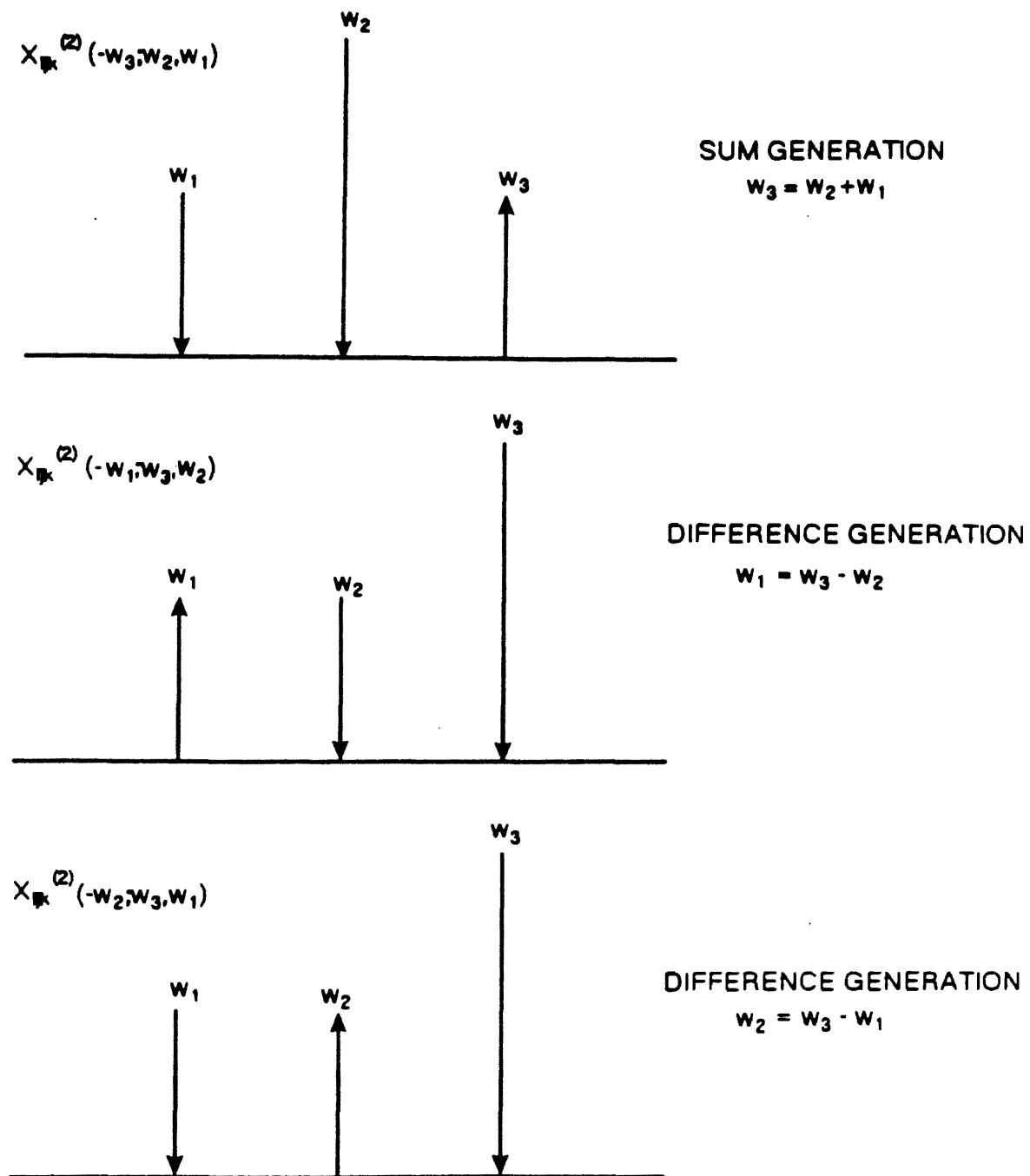DIFFERENCE GENERATION

$w_2 = w_3 - w_1$

Figure 2. Three-Wave Mixing

$$\frac{dE_1(z)}{dz} = -i \frac{8\pi\omega_1{}^2}{k_1 c^2} dE_1^*(z) E_2(z) e^{-i\Delta kz}$$

$$\frac{dE_2(z)}{dz} = -i \frac{16\pi\omega_1{}^2}{k_2 c^2} dE_1^2(z) e^{-i\Delta kz} \tag{5.1}$$

where $\omega_2 = 2\omega_1$ and $\Delta k = 2k_1 - k_2$

The second harmonic power for small signal approximation is given by

$$S(2\omega) = \frac{512\pi^5 d^2 L^2 S^2(\omega)}{n(2\omega) n^2(\omega) \lambda^2 c} \left(\frac{\sin x}{x}\right)^2 \tag{5.2}$$

where λ is the wavelength of the fundamental and $x = \Delta kL/2$

The power flow is given by

$$W = \frac{k_1 c^2}{8\pi\omega_1{}^2} \varepsilon_1{}^2(z) + \frac{k_2 c^2}{16\pi\omega_2{}^2} \varepsilon_2{}^2(z) \tag{5.3}$$

Solution of these equations was first worked out by Bloembergen and co-workers [3]. For a simplified case, we consider a phase matched case for which the initial second-harmonic power is zero (i.e. $\Delta k = 0$ and $\varepsilon_2(0) = 0$)

The solutions obtained are as follows [26] :

$$E_{R_2}(L) = E_{R_1}(0) \tanh\frac{L}{l_{SH}} \tag{5.4}$$

$$E_{R_1}(L) = E_{R_1}(0) \operatorname{sech}\frac{L}{l_{SH}} \tag{5.5}$$

where

$$I_{SH} = (\frac{4\pi\omega^2 d}{k_1 c^2} E_{R_1}(0))^{-1} \qquad (5.6)$$

It implies from the equation 5.2 that if we had a sufficiently long pathlength, a high degree of second-harmonic conversion could be achieved, regardless of how small the d coefficient might be. But this is not true for practical cases, due to its limitations. If the incident fundamental beam is focussed, the input angle θ will not be a discrete value, but an envelope centered at θ. Therefore the phase matching condition will be limited to some finite length in the crystal.

Another important limitation on the interaction length is due to a phenomenon called walkoff. In general, ordinary and extraordinary waves propagate in slightly different directions in birefringent media. The reason for this being the different polarization of the media along the e(z) principal axis by e(θ) wave. Due to this the power flow is bent slightly from that associated with the 0-wave. For θ = 90, the walkoff angle is zero. For any other angle, the angle is given by [14]

$$\rho \approx \tan\rho = \frac{n_e(\omega)}{2}(\frac{1}{(n_e(2\omega)^2)} - \frac{1}{(n_o(2\omega))^2})\sin 2\theta \qquad (5.7)$$

5.3 Parameters Affecting The Doubling Efficiency

The efficiency of the conversion of second-harmonic generation is dependent on two categories of parameters. The first one consists of the parameters which are related to the laser source. The second class has the parameters associated with the harmonic generator.

The first class has the parameters such as power density, beam divergence, spectral linewidth and spectral brightness. The conversion efficiency is proportional to the power density of the fundamental beam, where as the harmonic power itself is proportional to the product of fundamental power and power density. The conversion efficiency also changes due to the beam divergence. When collinear phase matched second-harmonic generation is used, the two light waves may have a finite divergence. This would introduce a mismatch in the wave vector. If $\delta\theta_m$ is the deviation from the perfect phase matching angle, then the beam divergence $\Delta\theta$ at which the conversion efficiency drops to one half of its peak value is given by [14] :

$$\Delta\theta = \frac{0.44\lambda_1 \frac{n_1^{\,0}}{l}}{(n_2^{\,0} - n_2^{\,e})\sin2\theta_m} \tag{5.8}$$

with $\Delta\theta = 2n_1\delta\theta$

The deviation in wavelength from the central wavelength λ_0 at which the perfect phase matching occurs also reduces the conversion efficiency.

If $\delta\lambda = \lambda - \lambda_0$ and $\Delta\lambda = 2\delta\lambda$, then the spectral linewidth at which the doubling efficiency drops to one half is given by [14]

$$\Delta\lambda = \frac{0.44\lambda_1}{l}\left(\frac{\partial n_1^{\,0}}{\partial\lambda_1} - \frac{1}{2}\frac{\partial n_2^{\,e(\theta)}}{\partial\lambda_2}\right) \tag{5.9}$$

Thus, it is evident that for a high conversion efficiency, the laser source should have a high power density, small beam divergence and a narrow linewidth. These three properties can be merged into a single parameter called spectral brightness. For high efficiency second-harmonic generation the laser should exhibit a high spectral

brightness, which can be achieved by transverse and longitudinal mode selections.

The second class consists of parameters such as temperature, phase matching angle, absorption, optical homogeneity, nonlinear coefficient and figure of merit of the crystal. The temperature changes of the doubling crystal are caused due to the variations in the room temperature and due to the absorption losses in the crystal. The expression for the temperature sensitivity of the doubling crystal with respect to second-harmonic generation is given by [14]

$$\Delta T = \frac{0.44\lambda_1}{ld(n_2{}^e - n_1{}^0)/dT}$$ (5.10)

where $\Delta T = T - T_0$

ΔT is defined as the full width at half-maximum of the temperature range over which second-harmonic generation is possible in a particular crystal. The phase-matching angle is a very important parameter to be considered, since it indicates the angular range in which the crystal can be titled to give a sufficient second-harmonic generation. The doubling efficiency is also affected by the absorption in the crystal. This will introduce thermal gradients and thermally introduced stresses. This further affects the refractive index of the crystal which makes the phase-matching task more difficult. Optical homogeneity is hence another important aspect since any index inhomogeneities would reflect the same problems. Thus we find that damage threshold, optical quality, angular and thermal tuning range and acceptance angle are important parameters. The equally important parameter is nonlinear coefficient. And there is a trade off necessary with the interaction length, to achieve the best second-harmonic

generation conversion efficiency. Hence, all these above parameters are combined to give a figure of merit, which characterizes either the laser source or the crystal or both.

5.4   Intracavity Frequency Doubling

Usually, the frequency doubling experiments have a nonlinear crystal placed in the output beam of a laser system. But this arrangement does not work efficiently for a CW-pumped laser system. For a high second-harmonic conversion efficiency, the power density of the laser system should be high, which is not true for the above mentioned system. To avoid this, the concept of intracavity doubling was introduced. The nonlinear crystal when placed inside the laser resonator, the circulating power would increase by a factor of 1/T higher than the output power. In such a cavity, the output mirror with transmission T is replaced by one which is 100% reflective at the fundamental and completely transmitting at the second-harmonic. In such a system the nonlinear crystal inside the laser couples out power at twice the laser frequency, unlike the normal lasers in which the mirror couples out power at the laser frequency. This gives a high power density inside the cavity and thus eliminates the CW-pumped laser system drawback.

Apart from this major advantage, the system has a few disadvantages. The quality of the nonlinear crystal is very important. A crystal of poor quality would drastically degrade the performance of the laser. Any fluctuations of the amplitude would be amplified too in the gain medium. For a standing wave cavity the harmonic

power is generated in two directions, hence a dichroic mirror is needed to combine these two beams. There are other means like using the external doubling with a strongly focussed beam, but this requires a very high power density, which can damage the crystal.

5.5 Parametric Process

Sum and Difference frequency generation are two of the most important parametric processes. Especially, second-harmonic generation is a special case of sum frequency generation process.

5.5.1 Sum-Frequency Generation

According to the Manley-Rowe relations, for sum-frequency generation the power is lost by the pumping laser frequencies at ω_1 and ω_2 and gained by the sum frequency [26]. In this process, two beams similar in power are directed into a nonlinear medium with the power generated at the sum frequency.

$$P_3 = \frac{512\pi^5 d^2 P_1 P_2}{n_1 n_2 n_3 \lambda_3^2 c} \left(\frac{\sin x}{x}\right)^2 \tag{5.11}$$

Here, the output power is again proportional to the input powers. The concept of phase matching becomes more complicated since it requires the knowledge of refractive indices at three different frequencies.

5.5.1.1 Parametric Up-Conversion. When one of the source frequencies for a set up of sum-frequency generation is much more intense than the second frequency

ω_1, the process generated is known as parametric up-conversion. Such an intense source is known as the pump. The output power at the beginning for such a case is zero. If ω_2 is the pump, the energy depleted from ω_2 is very small. Hence in the equations 3.29, dE_2/dz can be put as zero. Then the following solution is obtained [26]:

$$E_3(Z) = \sqrt{\frac{\omega_3{}^2 k_1}{\omega_1{}^2 k_3}} E_1(0) \sin\frac{z}{1_p} \qquad (5.12)$$

where

$$1_p = \left(\frac{4\pi d}{c^2}\sqrt{\frac{\omega_1{}^2\omega_3{}^2}{k_1 k_3}}E_2\right)^{-1} \qquad (5.13)$$

and

$$E_1(Z) = E_1(0)\cos\frac{z}{1_p} \qquad (5.14)$$

where $E_1(0)$ is incident amplitude of the weak field.

It is found that the intensity of the weak photon can be shifted to a new frequency ω_3 where it might be detected more efficiently. Detectors in the visible region are more efficient than in those in the infrared region making this process very suitable for spectroscopic applications.

5.5.1.2 Difference-Frequency Generation. In this type of parametric process, if $\omega_3 - \omega_2 = \omega_1$ is the equation of interest, then power is lost not only to the generated frequency at ω_1 but also to the source at ω_2. This could be described as the splitting of

a photon at ω_3 into two photons at ω_1 and ω_2. We find that if a weak signal at a lower frequency is made to interact with the highest frequency signal (ω_3), then a frequency at ω_1 is created and signals at lower frequencies are amplified. Here ω_3 is defined as pump, and the generated signal ω_1 is known as idler, while ω_2 becomes the source in this case.

If ω_3 is the pump frequency incident on a second-order nonlinear material, then the output will have two frequencies ω_1 and ω_2 for which

$$\omega_1 + \omega_2 = \omega_3$$

$$\text{and} \quad k_1 + k_2 \approx k_3$$

Thus, we get many pairs of ω_1 and ω_2 which satisfy the above condition. This phenomenon is known as parametric fluorescence.

5.6 Multimode Spectrum And Intensity Fluctuations Phenomena

A very small proportion of lasers in use today operate in a true single mode, i.e. with a single frequency and a wavefront with a Gaussian intensity profile. Most lasers have the Gaussian intensity profile of the TEM_{00} mode, but their frequency spectrum indicates that they produce a series of discrete frequencies spaced by $c/2L$ Hz, where c is the velocity of light, and L is the length of the laser resonator. In general, for each of these longitudinal modes there are a number of transverse modes and the intensity profile of the output is not Gaussian nor does it have a simple phase distribution across it. Such complex frequencies and phase distributions of the available power have a surprising effect upon the conversion efficiency during the

Second-Harmonic generation and other optical mixing processes.

The time output of a multimode laser looks noiselike, but has a repetitive structure that repeats every 2L/c sec and only changes its detailed form over many cycles as the relative phases of the modes drift. The incident beam is composed of a number of sinusoidal waves whose amplitudes and phases are random variables. They are not necessarily statistically independent. The nonlinear processes will couple different modes and may establish partial or complete correlation between them. The Second-Harmonic Generation process gains more from the peaks of this noiselike waveform than it loses from the troughs, and on an average, a gain in conversion is obtained. For Sum and Difference-frequency generation, the random nature of the amplitude and the phase of both different fields result in a mismatch indicating the non-overlap of the peaks, resulting in low conversion efficiency. This is shown in Figures 3 and 4.

Nonlinear processes absorb and attenuate a light beam in a different way from that due to a linear process. For a nonlinear process the absorption law is dependent on the instantaneous intensity. As a result there is not only a change in the mean intensity of the beam but also the spatial profile of the beam, the light fluctuations and spectrum of the light modify. These significantly alter the properties of the incoming beam.

The fluctuations are characterized by the intensity correlation function $g^{(2)}(0)$. The normalized intensity correlation function is given by [24]
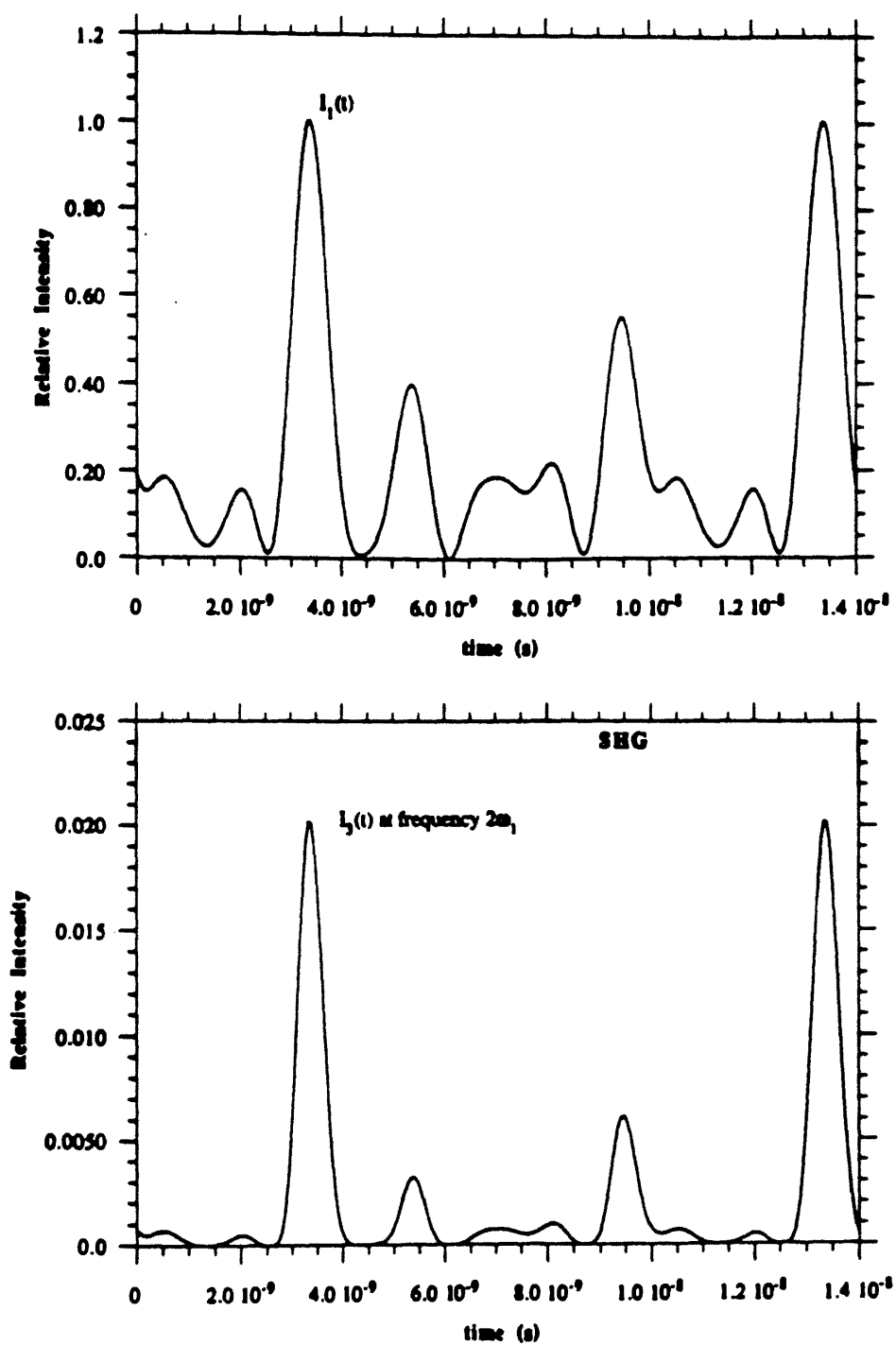
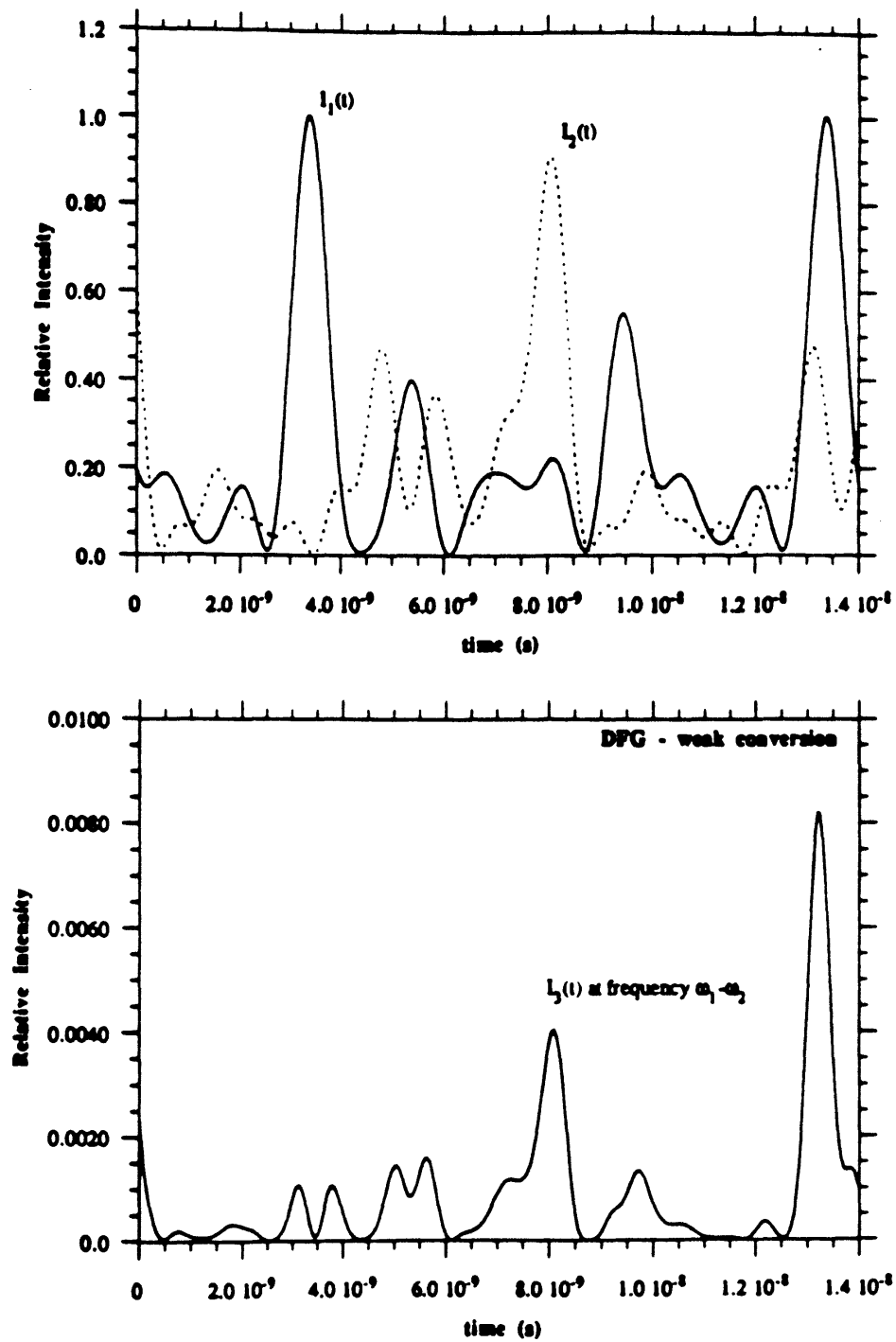Figure 3. Second-Harmonic Generation for Multimode Laser [19]

Figure 4. Difference-Frequency Generation for Multimode Laser [19]

$$g^{(0)}(\tau) = \langle I(t)I(t+\tau)\rangle / \langle I\rangle^2 \qquad (5.15)$$

where $< I >$ is the average intensity.

This function is a measure of how strong the relative fluctuation of a signal is. According to the Weiner-Khintchine theorem [24], the unnormalized auto-correlation function $G^{(2)}(\tau)$ is the Fourier transform of $|I(\theta)|^2$, where $I(\theta)$ denotes the Fourier spectrum of the intensity $I(t)$.

For a multimode laser with independently oscillating modes or for the light from a thermal source transmitted through a narrow band optical filter, $g^{(2)}(0) = 2$. For a mode locked laser $g^{(2)}(0)$ takes a value of the order of magnitude of the number of the coupled modes, while for a beam of constant intensity like a coherent beam or a frequency modulated beam of constant intensity, $g^{(2)}(\tau) = 1$ for all τ.

Figure (5) shows the fluctuations of a beam for different amounts of Two Photon Absorption. The instantaneous intensity of a beam with modes oscillating simultaneously, but independently of each other is shown in part (a). $< I_0 >$ indicates the mean incident laser intensity, β is the nonlinear absorption coefficient, while z is the path length. Ω is the beat frequency of adjacent modes and $< I >$ is the mean intensity of the transmitted beam. The plots were taken for 30 equidistant modes of equal intensity and random relative phases.

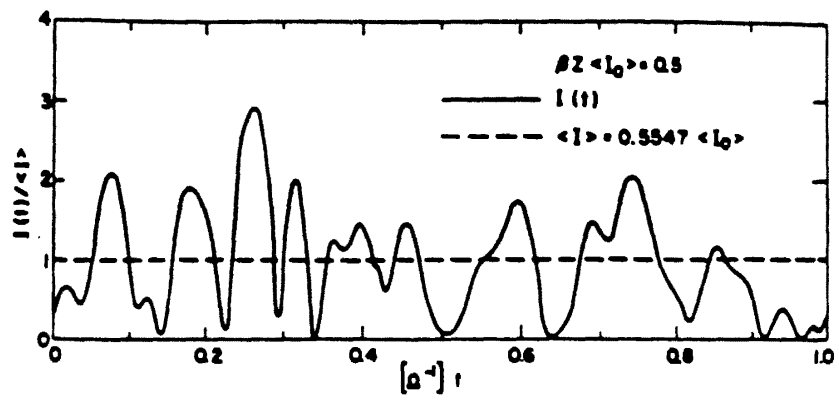For $\tau = 0$, equation 5.15 becomes

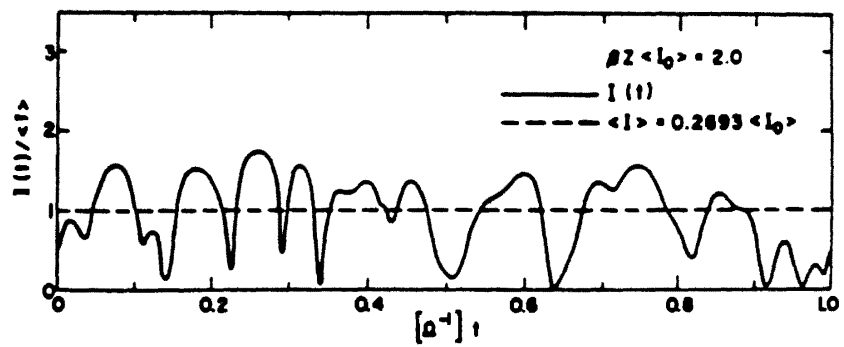$$g^2(0) = \langle I^2\rangle / \langle I\rangle^2 \qquad (5.16)$$

Here $< I^2 >$ gives the relative strength of the second-harmonic generation.
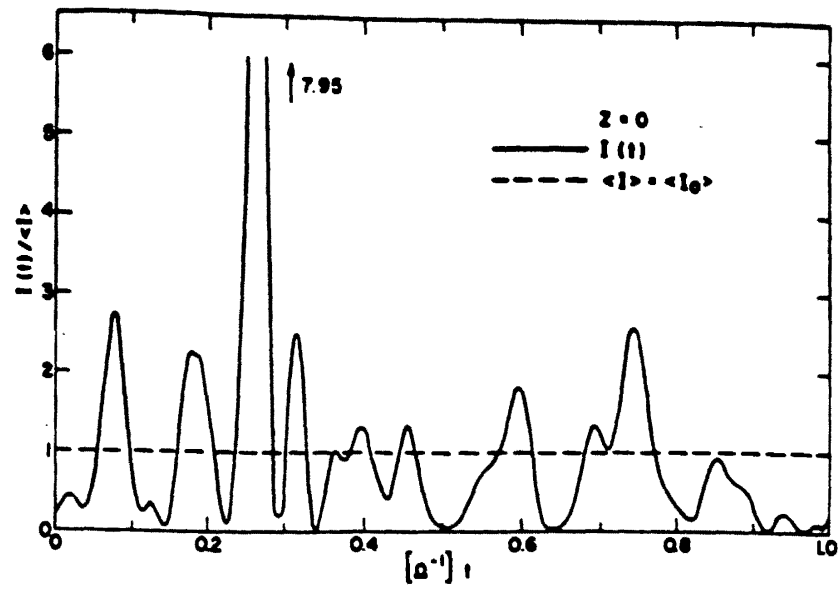
Figure 5. Fluctuations of a Multimode Laser Beam [24]

The plot indicates that the fluctuations reduce as the beam propagates through the media. But this modifies the light spectrum and light is created outside the range of the original spectrum. As seen in part (c), the changes around the intensity minima are much faster compared to those of part (a). This is possible due to an increase in the linewidth. The repetition rate of the deep minima is found to be the same, corresponding to the original bandwidth. The intensity peaks are very much reduced compared to the mean intensity. These two point indicate that the output of a nonlinear process is very comparable to an FM signal, with random frequency modulation.

This means that if a beam is transmitted through a suitable dispersive medium large random fluctuations with repetition corresponding to the bandwidth of the new spectrum will reappear. Thus, the spectrum of light is modified.

The multimode structure also has a great effect on the generation of beat frequencies. Consider first the influence of temporal coherence in two beams with N_1 and N_2 frequency components respectively centered around ω_1 and ω_2. Each component of the first beam will beat with each component of the second beam to give a difference near $\omega_2 - \omega_1$. The bandwidth of the detection system at the frequency $\omega_2 - \omega_1$ will determine how many of these $N_1 N_2$ beats will contribute to the signal. If the bandwidth of the detector is smaller than the equal spacing between the individual N components in each light beam, the resultant signal at $\omega_2 - \omega_1$ will be reduced by a factor equal to the larger number N_1 or N_2, compared to the signal produced by two purely monochromatic light beams of the same intensity. The spatial coherence effect is also similar.

The temporal dependence of the multimode input field is given by [19]

$$E_i(0,\tau) = \sum_{-n}^{n} jE_{ij}\exp(i(\omega_{ij}\tau+\theta_{ij}))$$

$$= \exp(i(\omega_i\tau))\sum_{-n}^{n} jE_{ij}\exp(i(j\Delta_i\tau+\theta_{ij}))$$

for i = 1, 2

where $\omega_{ij} = \omega_i + j\Delta_i$ is the central frequency of the ith field, Δ_i is the mode frequency spacing of cavity i, and θ_{ij} are randomly chosen phases for different modes.

The reduction factor does not apply for d.c. rectification of light. In that case each mode can beat with itself to give a d.c. voltage proportional to the integrated fundamental frequency, regardless of the mode distribution.

5.7 Sum-Frequency Generation With Improved Efficiency

An experiment to increase the efficiency of sum-frequency generation for broadband input fields performed in our laboratory by Dr. C. Radzewicz, Dr. J. S. Krasinski and Dr. Y. B. Band is described in details in this section [19]. This innovative method uses two or more nonlinear crystals, with a variable time delay between them to temporally shift the fundamental fields one relative to another by a time longer than their coherence time. This method succeeded in increasing the efficiency of sum-frequency generation considerably, but not the difference-frequency efficiency.

The most important requirement for higher efficiency is proper spatial and temporal overlap. For broadband fields, it becomes very difficult to have the intensity

of both the beams high at the same instant. The conversion efficiency for second-harmonic generation is always greater than that for sum-frequency generation, since for second-harmonic generation both the waves are identical by definition and generated from the same source. Hence they have high intensity at the same time giving very high conversion efficiencies.

For sum-frequency generation two different and noncorrelated lasers are used as light sources. The uncorrelated fluctuations result in substantial decrease of efficiency.

As it was discussed before, the intensity auto-correlation function for a multimode laser is $g^2(0)=2$. For two uncorrelated multimode lasers the cross-correlated function is $g^2(0)=0.5$. This shows that in low conversion limit efficiency of sum-frequency generation is four times less than that of second harmonic generation. For higher conversion the situation is even worse since very few overlapping fluctuations of intensity are quickly depleted and in result two auto-correlated beams are formed at the input frequencies. In such beams there is very little phase overlap and conversion efficiency approaches zero.

The experiment described below tries to eliminate this overlap problem for a sum-frequency generation. The spatial overlap is achieved for TEM_{00} fields by aligning the centers of the two input beams and using beams with the same beam diameter and divergence. The temporal overlap is automatic for single longitudinal mode beams, and can be achieved for pulsed beams by overlapping the peaks of the pulses with identical profiles.

The experimental set up is shown in fig.(6). The two input beams for sum-frequency generation were generated in excimer laser pumped dye lasers. The gas mixture used for the excimer was XeCl [Xenon Chloride]. This is a poisonous gas, and proper ventilation was provided for safety reasons. The Lambda- Physik excimer was cooled by using purified and cooled running water. The laser output from the excimer at a wavelength of 308 nm was focussed on the two Molectron DL200 dye lasers, using a beam-splitter. Each of these dye lasers consisted of an oscillator and an amplifier. The dye solutions used were Coumarin 480 and Rhodamine 6G generating light at 480 and 575 nm respectively. The output beams from the oscillators were spatially filtered and amplified using prism cells of Bethune design to achieve high quality optical beams. The maximum output energy from the amplifiers was about 2mJ and had a pulse duration of 10 ns. The bandwidth of the lasers were approximately 7 GHz and mode spacing was 375 MHz. The oscillator and the amplifiers were never allowed to saturate during the experiment. The lasers were nearly free of nonlinear mode coupling and had several independent modes with random phases.

These two horizontally polarized ω_1 and ω_2 beams were combined by a Pellin-Broca Prism P1 and focussed by a 1m focal length lens L1 into the type I BBO nonlinear crystal of 6mm length. The output from this crystal consists of frequency components at ω_1 , ω_2 and $(\omega_1 + \omega_2)$. This output is recollimated by lens L2 and separated into spectral components by a prism P2. The sum frequency intensity at 262 ns was measured by detector D1. A range of different conversion efficiencies was measured using different intensities of ω_1 beam. The maximum conversion efficiency
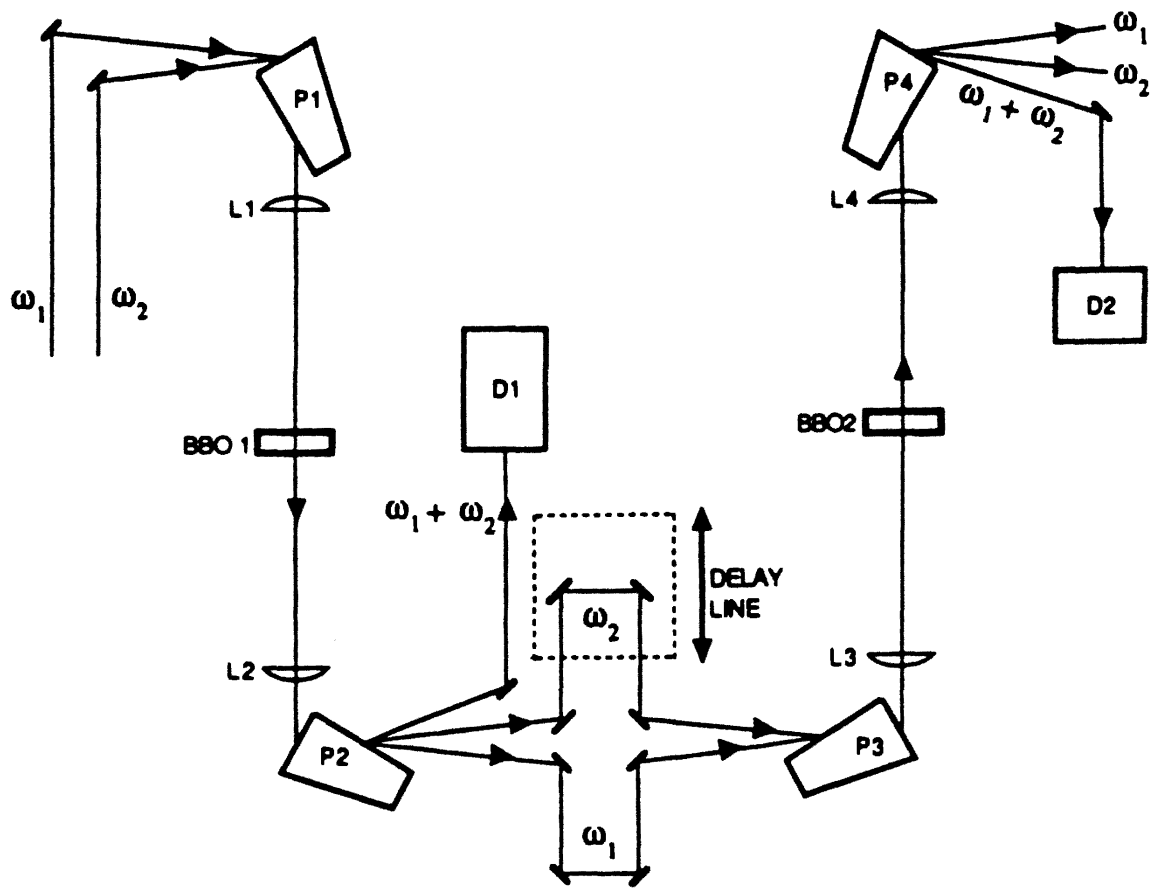
Figure 6. Experimental Set Up [19]

for the first crystal was found to be 15%. Now the concept of time delay was introduced between the beams ω_1 and ω_2. There was a variable time delay arrangement set up in the path of the beam at ω_2. A d.c. motor was used for the smooth motion of the prism and the length to be adjusted was controlled by a software written in GWBASIC on a computer. The interface was done using a GPIB card. The modified ω_2 and unaltered ω_1 were again combined by a prism P3 and were focussed by a lens L3 into a second identical nonlinear crystal, and the output was again recollimated by lens L4 and separated into spectral components by means of a prism P4. The sum-frequency $(\omega_1 + \omega_2)$ was this time measured by detector D2. The walk-off of ω_3 from ω_1 and ω_2 beams in BBO1 and BBO2 was substantial which partially avoided the reconversation of ω_3 photons back to the fundamental beams.

The plot of the sum-frequency generation efficiency of the second nonlinear crystal versus the time delay τ between the ω_1 and ω_2 beams is shown in figure (7). The data are normalized to unity for time delay $\tau = 0$. The four different curves depict the corresponding conversion efficiencies of the first crystal η_1. It is found that η_2 increases with $|\tau|$. The width of the curves is comparable to the coherence time of the laser beams. For a time delay much higher than the coherence time the efficiency η_2 reaches a constant value for a particular value of η_1. Conversion increment of as high as 70% was observed over that of one at $\tau = 0$ for $\eta_1 = 15\%$. For very high time delays $\eta_1 \approx \eta_2$ can be achieved.

Thus, as explained in the beginning of this section, the efficiency of Sum-Frequency Generation in the first crystal at any moment of time, increases with the

product of instantaneous intensities of the ω_1 and ω_2 beams. Both the lasers have their intensities fluctuating randomly, and the first nonlinear crystal practically eliminates these mutually correlated intensity fluctuations converting them into sum frequencies. The laser beams after this are anti-correlated in the time domain. This would reduce the conversion efficiency in the second crystal. But when a delay τ is introduced which is longer than the coherence time, the anti-correlation is destroyed and the efficiency in the second crystal builds up. This is observed in figure (7) where the efficiency is low at $\tau = 0$, because of this anti-correlation which in turn reduces the conversion efficiency.

This method demonstrates the solution for increasing the efficiency of the sum-frequency generation. It shows that the conversion efficiency can be made as high as the conversion efficiency of the first crystal. This experiment has shown only two stages of nonlinear crystals, but this could be further extended by cascading more stages.
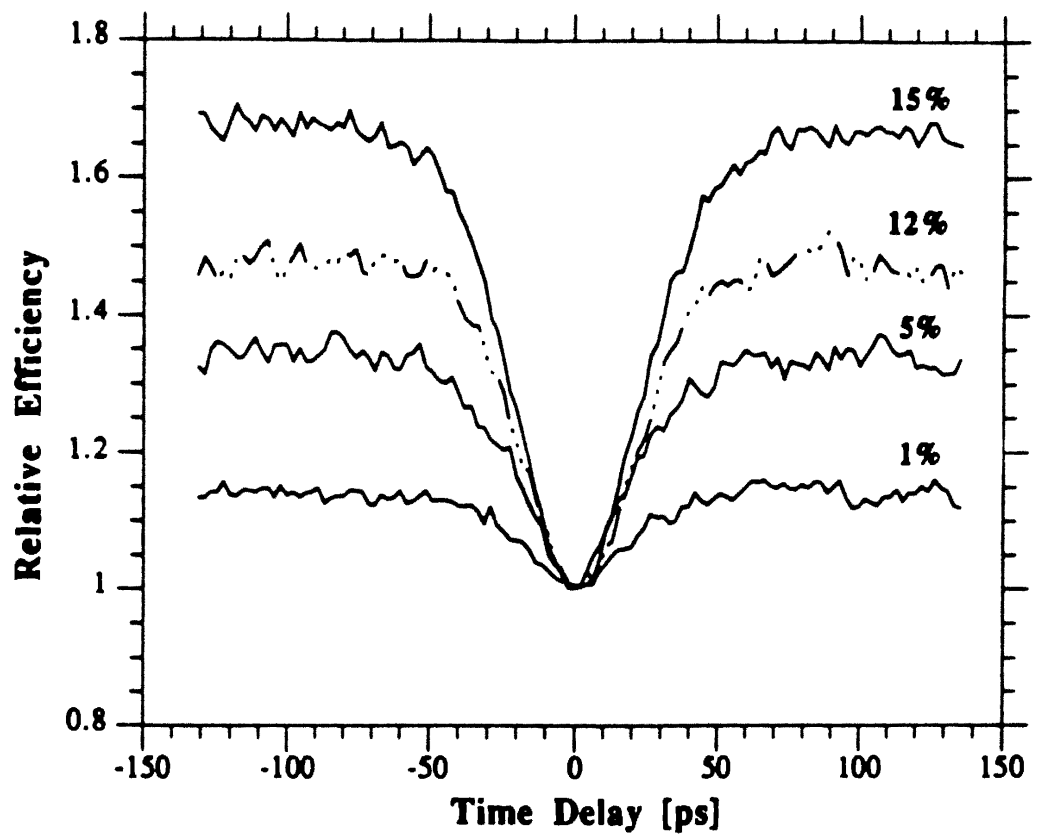
Figure 7. Improvement in efficiency in second crystal (η_2) versus time delay (τ) [19]

CHAPTER VI

SUMMARY AND CONCLUSIONS

The field of nonlinear optics is very vast. There are many branches of nonlinear

optics which are still to be explored. Here an attempt was made to cover one such

field of generating efficiently the second harmonic and sum frequencies. The basics of

linear optics was discussed to lay a basis for nonlinear optics. The important concepts

of nonlinear optics were discussed and derived where necessary. These theoretical

concepts help to lay a foundation for higher level research.

An experiment to increase the efficiency of sum-frequency generation using

broadband inputs was described and analyzed. An understanding of multimode

spectrum of lasers and its effects on frequency conversion efficiencies was given. The

experiment demonstrated that the efficiency of second harmonic generation is always

higher than that of sum or difference generation process. But this experiment

successfully indicated that the sum-frequency efficiency can be increased significantly

using an arrangement with two or more nonlinear mixing crystals. The experiment

utilized time delay line situated between the crystals, for one of the fundamental fields

relative to the other. The delay line helped to temporally shift the fundamental fields

one relative to another by a time longer than their coherence time. The conversion

efficiency of the second crystal was increased almost to that of the first crystal by

eliminating the anti-correlation caused by the sum-frequency generation in the first crystal.

Thus it could be concluded that if it was possible to generate higher conversion efficiencies by the method described here. Since there is lots of indepth research still needed in this area of nonlinear optics, it would always prove to be an exciting and rewarding experience for all enthusiastic students and capable researchers.

BIBLIOGRAPHY

1. Armstrong, J. A., Bloembergen, N., Ducuing, J., and Pershan, P. S., "Interactions Between Light Waves in a Nonlinear Dielectric," Phys. Rev., 127, pp. 1918, 1962.

2. Ashkin, A., Boyd, G. D., and Kleinman, D. A, "Phasematched Second Harmonic Generation without Double Refraction," Appl. Phys. Lett., 6, pp.179, 1965.

3. Bloembergen, N., Nonlinear Optics, W. A. Benjamin, Inc., 1977.

4. Born, M.,Wolf, E., Principles of Optics, Pergamon Press, 6th ed., 1983.

5. Boyd, G. D., and Patel, C. K. N., "Enhancement of Optical Second Harmonic Generation (SHG) by Reflection Phase Matching in ZnS and GaAs." Appl. Phys. Lett., 8, pp. 313, 1966.

6. Chemla, D. S., and Zyss, J., Nonlinear Optical Properties of Organic Molecules and Crystals, Vol. 1, Academic Press, Inc., 1987.

7. Dmitrev, V. G., Gurzadyan, G. G., and Nikogosyan, D.N., Handbook of Nonlinear Optical Crystals, Springer-Verlag, 1991.

8. Fincham, W. H. A.,and Freeman, M. H., Optics, Butterworths, 9th ed., 1980.

9. Flytzanis, C., and Oudar, J. L., Nonlinear Optics: Materials and Devices, Springer-Verlag, 1986.

10. Gupta, S., Arora, D., Sarna, S. B., and Lonkar, P., Microwave Fundamentals, Khanna Publishers, 1989.

11. Haus, H. A., Waves and Fields in Optoelectronics, Prentice-Hall, Inc., 1984.

12. Hayes, W., and Loudan, R., Scattering of Light by Crystals, John Wiley & Sons, 1978.

13. Jordan E. C., and Balmain, K. G., Electromagnetic Waves & Radiating Systems, Prentice-Hall, Inc., 2nd ed., 1987.

14. Koechner, W., Solid-State Laser Engineering, Springer-Verlag, 2nd ed., 1988.

15. Kurtz, S. K., and Perry, T. T.,"A Powder Technique for the Evaluation of Nonlinear Optical Materials," Journal of Appl. Phys., 39, pp. 3798, 1968.

16. Maker, P. D., Terhune, R. W., Nisenoff, M., and Savage, C. M., "Effects of Dispersion and Focusing on the Production of Optical Harmonics." Phys. Rev. Lett., 8, pp. 21, 1962.

17. Minck, R. W., and Wang, C. C., "Nonlinear Optics," Proceedings of the IEEE, Vol. 54, no. 10, pp. 1357-1374, 1966.

18. Prasad, P. N., and Williams, D. J., Introduction to Nonlinear Optical Effects in Molecules and Polymers, John Wiley & Sons, 1991.

19. Radzewicz, C., Kransinski, J. S., and Band, Y. B., "Increased Efficiency for Sum Frequency Generation for Broadband Input Fields," (to be published).

20. Schubert, M., and Wilhemi, B., Nonlinear Optics and Quantum Electronics, John Wiley & Sons, 1986.

21. Shen, Y. R., The Principles of Nonlinear Optics, John Wiley & Sons, p. 1, 1984.

22. Skobel'tsyn, A. D. V., Nonlinear Optics , Consultants Bureau, 1970.

23. Wartikar, P. N., and Wartikar, J. N., A Text Book of Applied Mathematics, vol. I, II, Pune Vidyarthi Griha Prakashan, 9th ed., 1984.

24. Weber, H. P., "Two-Photon-Absorption Law a for coherent and Incoherent Radiation,"IEEE Journal of Quantum Electronics, Vol. QE-7, no. 5, pp. 189-195, 1871.

25. Yariv, A., Quantum Electronics, John Wiley & Sons, 3rd ed., 1989.

26. Zernike, F., and Midwinter, J. E., Applied Nonlinear Optics, John Wiley & Sons, 1973.

APPENDIX

NONLINEAR OPTICAL PROPERTIES OF CRYSTAL

The nonlinear optical properties of classical and recent uniaxial as well as biaxial crystals are given in this appendix [6, 7, 9, 14, 26].

Uniaxial Crystals

1. KH_2PO_4, Potassium Dihydrogen Phosphate (KDP)

This crystal was initially used for ultrasonic transducers and as an electrooptic material. This crystal is stable and can be heated and cooled. It is resistant to laser damage due to high or continuous powers. These crystals are easy to grow. But they have a poor infrared transmission and have fairly low refractive indices giving low nonlinear coefficients.

Specifications :

Negative uniaxial crystal : $n_o > n_e$

Point group : $\bar{4}2m$

Transparency range : 0.1765 - 1.7 μ

Dispersion relations (T = 24.8°C , λ in μm)

$$n_0{}^2 = 2.259276 + \frac{0.01008956}{\lambda^2 - 0.012942625} + \frac{13.00522\lambda^2}{\lambda^2 - 400}$$

$$n_e{}^2 = 2.132668 + \frac{0.008637494}{\lambda^2 - 0.012281043} + \frac{3.2279924\lambda^2}{\lambda^2 - 400}$$

2. KD_2PO_4, Deuterated Potassium Dihydrogen Phosphate (DKDP)

This is an isomorph of KDP normally known as KD*P. The reason for using

isomorph being the temperature dependence of their refractive indices allowing 90°

phase matching.

Specifications :

Negative uniaxial crystal : $n_o > n_e$

Point group : $\overline{4}2m$

Transparency range : 0.2 - 2.0 μ

Dispersion relations (T = 300°K , λ in μm)

$$n_0{}^2 = 1.661145 + \frac{0.586015\lambda^2}{\lambda^2 - 0.016017} + \frac{0.691194\lambda^2}{\lambda^2 - 30}$$

$$n_e{}^2 = 1.687499 + \frac{0.44751\lambda^2}{\lambda^2 - 0.017039} + \frac{0.596212\lambda^2}{\lambda^2 - 30}$$

3. $NH_4H_2PO_4$, Ammonium Dihydrogen Phosphate (ADP):

Similar to KDP,this crystal was also initially used as an electrooptic material.

But unlike KDP, this material decomposes when heated up to a temperature of 125°C.

It tends to crack when cooled. But it too is resistant to laser damage of both types. Its major disadvantages include poor infrared transmission and low nonlinear coefficients due to small refractive indices.

Specifications :

Negative uniaxial crystal : $n_o > n_e$

Point group : $\bar{4}2m$

Transparency range : 0.184 - 1.5μm

Dispersion relations (t=24.8°C, λ in μm)

$$n_0{}^2 = 2.302842 + \frac{0.011125165}{\lambda^2 - 0.013253659} + \frac{15.102464\lambda^2}{\lambda^2 - 400}$$

$$n_e{}^2 = 2.163510 + \frac{0.009616676}{\lambda^2 - 0.01298912} + \frac{5.919896\lambda^2}{\lambda^2 - 400}$$

4. $ND_4D_2PO_4$, Deuterated Ammonium Dihydrogen Phosphate (DADP) :

This is an isomorph of ADP, more commonly known as AD*P.

Specifications :

Negative uniaxial crystal : $n_o > n_e$

Point group : $\bar{4}2m$

Transparency range : 0.22 - 1.7 μm

Dispersion relations :   (λ in μm)

$$n_0{}^2 = 2.279481 + \frac{1.215879\lambda^2}{\lambda^2 - 57.975554333} + \frac{0.010761}{\lambda^2 - 0.013262977}$$

$$n_e^2 = 2.151161 + \frac{1.199009\lambda^2}{\lambda^2 - 126.6005279} + \frac{0.009652}{\lambda^2 - 0.009712103}$$

5. $LiIO_3$, Lithium Iodate :

This is a mechanically more stable material over a wide range of temperature from 20 - 256 °C. Its another advantage being freedom from degradation in a normal room environment. It does not have the refractive index damage problem that exists in Lithium Niobate and hence is more popular.

Specifications :

Negative uniaxial crystal : $n_o > n_e$

Point group : 6

Transparency range : 0.3 - 0.6 μm

Dispersion relations (λ in μm)

$$n_0^2 = 3.415716 + \frac{0.047031}{\lambda^2 - 0.035306} - 0.008801\lambda^2$$

$$n_e^2 = 2.918692 + \frac{0.035145}{\lambda^2 - 0.028224} - 0.003641\lambda^2$$

6. $LiNbO_3$, Lithium Niobate :

This is also known as Lithium meta-niobate. It offers several attractive features over ADP and KDP. It is nonhygroscopic and hard. Its mechanical stability is tolerable. It has a large nonlinear coefficient. Its temperature sensitivity is very useful

for phase matching procedures. But its major disadvantage was the damage effect. It shows this damage effect when illuminated by a continuous-wave gas laser. This was due to a slightly altered refractive index in the crystal, following the path of the laser beam. Due to this the crystal was not used for precise phase matching experiments.

Specifications :

Negative uniaxial crystal : $n_o > n_e$

Point group : 3m

Transparency range : 0.33 - 5.5 μm

Dispersion relations : (λ in μm , T in K)

$$n_o{}^2 = 4.9130 + \frac{0.1173 + 1.65 \times 10^{-8} T^2}{\lambda^2 - (0.212 + 2.7 \times 10^{-8} T^2)^2} - 2.78 \times 10^{-2}$$

$$n_e{}^2 = 4.5567 + 2.605 \times 10^{-7} T^2 + \frac{0.097 + 2.7 \times 10^{-8} T^2}{\lambda^2 - (0.201 + 5.4 \times 10^{-8} T^2)^2} - 2.24 \times 10^{-2} \lambda^2$$

7. β - BaB_2O_4, Beta - Barium Borate (BBO) :

Specifications :

Negative uniaxial crystal : $n_0 > n_e$

Point group : 3m

Transparency range at 0.5 level : 0.198 - 2.6 μm

Dispersion relations : (λ in μm)

$$n_0{}^2 = 2.7405 + \frac{0.0184}{\lambda^2 - 0.0179} - 0.0155 \lambda^2$$

$$n_e{}^2 = 2.3730 + \frac{0.0128}{\lambda^2 - 0.0156} - 0.0044\lambda^2$$

8. $Ag_3\ A_sS_3$, Proustite :

It has an exceptionally wide transmission band and the crystal is birefringent. It has comparatively high refractive index and hence shows large nonlinearity. The refractive index of Proustite is constant with respect to temperature. But one of the disadvantages of Proustite is that it is instable to high-power laser beams.

Specifications :

Negative uniaxial crystal : $n_o > n_e$

Point group : 3 m

Transparency range : 0.6 - 13 µm

Dispersion relations (λ in µm)

$$n_o{}^2 = 9.220 + \frac{0.4454}{\lambda^2 - 0.1264} - \frac{1733}{1000 - \lambda^2}$$

$$n_e{}^2 = 7.007 + \frac{0.3230}{\lambda^2 - 0.1192} - \frac{660}{1000 - \lambda^2}$$

9. α - SiO_2, Quartz :

This material was readily available in large, perfect, single crystals and is noncentrosymmetric and transparent for the interacting frequencies. This was the reason due to which Franken and his co-workers used quartz when they performed the

first experiment on Second-Harmonic Generation. Although quartz has very small

nonlinear coefficient, it is often used as a reference material for measuring the

parameters of other materials for which phase matching is not essential.

Specifications :

Negative uniaxial crystal : $n_e > n_o$

Point group : 32

Transparency range : 0.15 - 4.5 μm

Quartz exhibits optical activity.

If ρ is the polarization plane rotation angle in degree for the light propagating along

the optic axis in a crystal with length L =1 mm, then

$$\rho = -2.1 + \frac{8.14}{\lambda^2}$$

Biaxial Crystals

1. $KB_5O_8 . 4H_2O$, Potassium Pentaborate Tetrahydrate (KB5)

Specifications :

Positive Biaxial crystal : $2V_z = 126° 20'$ (λ in μm)

Point group : mm2

Transparency range : 0.165 - 1.4 μm

Dispersion relations (λ in μm)

$$n_x{}^2 = 1 + \frac{\lambda^2}{0.848117\lambda^2 - 0.0074477}$$

$$n_y{}^2 = 1 + \frac{\lambda^2}{0.972682\lambda^2 - 0.0087757}$$

$$n_z{}^2 = 1 + \frac{\lambda^2}{1.008157\lambda^2 - 0.009405}$$

2. $KB_5O_8 \cdot 4D_2O$, Deuterated Potassium Pentaborate Tetrahydrate (DKB5) :

Specifications :

Positive Biaxial crystal

Point group : mm2

Transparency range : 0.1625 - 1.9 μm

Dispersion relations (λ in μm)

$$n_x{}^2 = 1 + \frac{\lambda^2}{0.84857\lambda^2 - 0.0075428}$$

$$n_z{}^2 = 1 + \frac{\lambda^2}{1.0123\lambda^2 - 0.0095376}$$

3. LiB_3O_5 , Lithium Triborate (LBO) :

Specifications :

Negative Biaxial crystal

Point group : mm2

Transparency range : 0.16 - 2.6 μm

Dispersion relations (λ in μm)

$$n_x{}^2 = 2.4542 + \frac{0.01125}{\lambda^2 - 0.01135} - 0.01388\lambda^2$$

$$n_y{}^2 = 2.5390 + \frac{0.01277}{\lambda^2 - 0.01189} - 0.01848\lambda^2$$

$$n_z{}^2 = 2.5865 + \frac{0.01310}{\lambda^2 - 0.01223} - 0.01861\lambda^2$$

VITA

Pranav B. Doshi

Candidate for the Degree of

Master of Science

Thesis: SECOND-HARMONIC GENERATION AND OPTICAL MIXING
PROCESSES

Major Field: Electrical Engineering

Biographical:

Personal Data: Born in Bombay, India, August 26, 1968, the son of Bharat
and Jyoti Doshi.

Education: Graduated from The New Era High School, Bombay, India, in
June 1984; received Bachelor of Engineering Degree in Electronics
Engineering from University of Bombay, India in December, 1990;
completed requirements for the Master of Science Degree at
Oklahoma State University in May, 1993.

Professional Experience: Research Assistant, Department of Electrical and
Computer Engineering, Oklahoma State University, May, 1991, to
May, 1992.